JOURNAL OF GEOPHYSICAL RESEARCH: ATMOSPHERES, VOL. 118, 5893–5911, doi:10.1002/jgrd.50472, 2013

Trends in ozone, its precursors, and related secondary oxidation products in Los Angeles, California: A synthesis of measurements from 1960 to 2010

Ilana B. Pollack,[1,2] Thomas B. Ryerson,[2] Michael Trainer,[2] J. A. Neuman,[1,2] James M. Roberts,[2] and David D. Parrish[2]

Received 14 March 2013; revised 3 May 2013; accepted 6 May 2013; published 13 June 2013.

[1] Decreases in ozone (O_3) observed in California's South Coast Air Basin (SoCAB) over the past five decades have resulted from decreases in local emissions of its precursors, nitrogen oxides ($NO_x = NO + NO_2$) and volatile organic compounds (VOCs). Ozone precursors have been characterized in the SoCAB with measurements dating back to 1960. Here we compile an extensive historical data set using measurements in the SoCAB between 1960 and 2010. Faster rates of decrease have occurred in abundances of VOCs ($-7.3 \pm 0.7\%\,yr^{-1}$) than in NO_x ($-2.6 \pm 0.3\%\,yr^{-1}$), which have resulted in a decrease in VOC/NO_x ratio ($-4.8 \pm 0.9\%\,yr^{-1}$) over time. Trends in the NO_x oxidation products peroxyacetyl nitrate (PAN) and nitric acid (HNO_3), measured in the SoCAB since 1973, show changes in ozone production chemistry resulting from changes in precursor emissions. Decreases in abundances of PAN ($-9.3 \pm 1.1\%\,yr^{-1}$) and HNO_3 ($-3.0 \pm 0.8\%\,yr^{-1}$) reflect trends in VOC and NO_x precursors. Enhancement ratios of O_3 to (PAN + HNO_3) show no detectable trend in ozone production efficiency, while a positive trend in the oxidized fraction of total reactive nitrogen ($+2.2 \pm 0.5\%\,yr^{-1}$) suggests that atmospheric oxidation rates of NO_x have increased over time as a result of the emissions changes. Changes in NO_x oxidation pathways have increasingly favored production of HNO_3, a radical termination product associated with quenching the ozone formation cycle.

Citation: Pollack, I. B., T. B. Ryerson, M. Trainer, J. A. Neuman, J. M. Roberts, and D. D. Parrish (2013), Trends in ozone, its precursors, and related secondary oxidation products in Los Angeles, California: A synthesis of measurements from 1960 to 2010, *J. Geophys. Res. Atmos.*, *118*, 5893–5911, doi:10.1002/jgrd.50472.

1. Introduction

[2] Ozone concentrations have decreased significantly since the 1960s in the California South Coast Air Basin (SoCAB), a region encompassing the Los Angeles urban area. Maximum 8 h average ozone mixing ratios measured basin wide and at individual surface monitoring network stations in the SoCAB decreased by about a factor of 3 (Figure 1; http://www.arb.ca.gov/adam/index.html) between 1973 and 2010. The observed decrease in ozone is attributed to decreases in local emissions of volatile organic compounds (VOCs) [*Warneke et al.*, 2012] and nitrogen oxides ($NO_x = NO + NO_2$) [*McDonald et al.*, 2012], the precursors to ozone formation. Reactions of hydrocarbons and carbon monoxide (CO) with hydroxyl radicals (OH), as shown in (R1) and (R2), initiate ozone formation chemistry [*Finlayson-Pitts and Pitts*, 2000; *Jacob*, 1999] through formation of peroxy radicals. Oxidation of NO by HO_2 or RO_2 via (R3)–(R5) then generates nitrogen dioxide (NO_2) and produces ozone following photolysis (R6) and reaction with molecular oxygen (R7).

$$HO + CO + O_2 \rightarrow HO_2 + CO_2 \quad (R1)$$

$$HO + RH + O_2 \rightarrow RO_2 + H_2O \quad (R2)$$

$$HO_2 + NO \rightarrow NO_2 + HO \quad (R3)$$

$$RO_2 + NO \rightarrow NO_2 + RO \quad (R4)$$

$$RO_2 + NO + O_2 \rightarrow R'CHO + NO_2 + HO_2 \quad (R5)$$

$$NO_2 + h\nu \rightarrow O + NO \quad (R6)$$

$$O + O_2 + M \rightarrow O_3 + M \quad (R7)$$

[3] Ozone precursors have been extensively studied over the years in the SoCAB. Some of the earliest measurements of NO_x, CO, and speciated VOCs in downtown Los

[1]Cooperative Institute for Research in Environmental Sciences, University of Colorado Boulder, Boulder, Colorado, USA.
[2]Chemical Sciences Division, NOAA Earth System Research Laboratory, Boulder, Colorado, USA.

Corresponding author: I. B. Pollack, Chemical Sciences Division, Earth System Research Laboratory, National Oceanic and Atmospheric Administration, 325 Broadway, MS R/CSD7, Boulder, CO 80305, USA. (ilana.pollack@noaa.gov)

2169-897X/13/10.1002/jgrd.50472

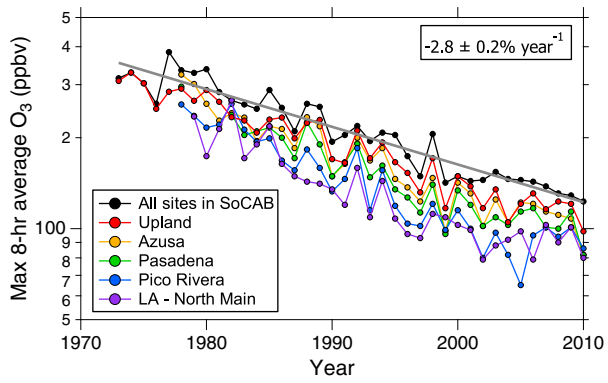

Figure 1. Maximum 8 h average ozone mixing ratios from selected Air Quality Monitoring District (AQMD) monitoring network stations in the SoCAB. Each data point represents the maximum 8 h average for a 1 year period. LLS fit of the maximum 8 h average for all sites in the SoCAB (solid gray line) indicates a decrease in ozone by a factor of 2.9 between 1973 and 2010, corresponding to a rate of decrease of $2.8 \pm 0.2\%\,\mathrm{yr}^{-1}$.

Angeles date back to 1960 [*Neligan*, 1962], after emissions from automobiles and local industry were identified as major contributors to photochemical smog [*Haagen-Smit*, 1952; *Haagen-Smit and Fox*, 1954]. These measurements initiated the development of an extensive surface monitoring network in the state of California and motivated future intensive field measurement campaigns. Since 1960, several short-term ground-based field studies have been conducted at selected locations within the SoCAB. Basin-wide measurements from instrumented research aircraft began in the 1970s [*Husar et al.*, 1977], and near-tailpipe measurements from mobile roadside monitors began in the early 1990s [*Beaton et al.*, 1995; *Bishop and Stedman*, 2008; *Gertler et al.*, 1999; *Lawson et al.*, 1990]. Long-term trends in ozone and emissions of its precursors in the SoCAB have been extensively studied using the data collected in these experiments [*Ban-Weiss et al.*, 2008; *Bishop and Stedman*, 2008; *Dallmann and Harley*, 2010; *Fortin et al.*, 2005; *Fujita et al.*, 2003; *Fujita et al.*, 2013; *Grosjean*, 2003; *Harley et al.*, 2005; *McDonald et al.*, 2012; *Parrish et al.*, 2002; *Parrish et al.*, 2011; *Warneke et al.*, 2012].

[4] Other secondary pollutants such as nitric acid (HNO_3), alkyl nitrates ($RONO_2$), peroxides (H_2O_2 and ROOH), and peroxyacetyl nitrate (PAN; $CH_3C(O)O_2NO_2$), formed in reactions accompanying those that produce ozone, have also been measured in the SoCAB. Formation of HO_x-NO_x oxidation products, such as nitrates via (R8) and (R9) and peroxides via (R10) and (R11), effectively removes these radicals from ozone-producing reaction cycles. In contrast, formation of VOC-NO_x oxidation products, such as PAN via (R12), produces temporary reservoir species for HO_x and NO_x due to relatively short thermal decomposition lifetimes for the peroxyacyl nitrates under surface conditions characteristic of summertime in Los Angeles [*Roberts et al.*, 2007; *Roberts et al.*, 1995; *Stephens*, 1969; *Grosjean et al.*, 2001; *Grosjean*, 2003; *Tuazon et al.*, 1991]. These reactions propagate the radical chain and lead to continued ozone production.

$$\mathrm{HO} + \mathrm{NO_2} \rightarrow \mathrm{HNO_3} \quad \text{(R8)}$$

$$\mathrm{RO_2} + \mathrm{NO} \rightarrow \mathrm{RONO_2} \quad \text{(R9)}$$

$$\mathrm{HO_2} + \mathrm{HO_2} \rightarrow \mathrm{H_2O_2} + \mathrm{O_2} \quad \text{(R10)}$$

$$\mathrm{RO_2} + \mathrm{HO_2} \rightarrow \mathrm{ROOH} + \mathrm{O_2} \quad \text{(R11)}$$

$$\mathrm{CH_3C(O)O_2} + \mathrm{NO_2} \rightarrow \mathrm{CH_3C(O)O_2NO_2} \quad \text{(R12)}$$

[5] The interdependence of these odd-hydrogen sinks with the chain reactions that produce ozone, reactions (R1)–(R7), makes the oxidation products of reactions (R8)–(R12) a useful tool for attributing a cause and effect relationship between decreasing ozone and decreasing precursor abundances [*Kelly*, 1992; *Roberts et al.*, 2007; *Roberts et al.*, 1995; *Sillman et al.*, 1990; *Sillman*, 1991; *Trainer et al.*, 1993]. Even though secondary oxidation products have been measured and studied in SoCAB field experiments since the 1960s and 1970s, relatively few peer-reviewed publications analyze these data over multiple years. These few include reviews of hydrogen peroxide (H_2O_2) measurements [*Lee et al.*, 2000; *Sakugawa et al.*, 1990], with several measurements in the California SoCAB between 1970 and 1988, and reports of ambient PAN measurements at various sites in the SoCAB between 1960 and 1997 by *Grosjean* [2003] and between 1975 and 1983 by *Temple and Taylor* [1983]. Historical analyses of secondary oxidation products other than ozone in the SoCAB have been largely neglected, despite their key role as indicators for understanding the response of ozone production rates and yields following changes in precursor emissions.

[6] In this work, we confirm and extend reported long-term trends in abundances and emission ratios of ozone precursors over the five decades from 1960 to 2010 in the SoCAB using data from surface monitoring network stations, mobile roadside monitors, ground-based field campaigns, and instrumented research aircraft. Abundances and emission ratios of ozone precursors determined from these measurements are also compared to those derived from emission inventories. We further report long-term trends in secondary oxidation product concentrations and extend the measurements to 2010. Measured abundances and enhancement ratios for secondary oxidation products are compared with values predicted by a chemical box model [*Fujita et al.*, 2013]. These long-term trends are described as exponential decreases [e.g., *Parrish et al.*, 2002; *Warneke et al.*, 2012] and quantified by calculating average rates of change per year. We use this approach to define trends in measured precursors and secondary pollutants. Correlations of ozone and related oxidation products with precursor abundances and VOC/NO_x ratio are identified using these historical data. Decadal changes in ozone production efficiency and rate of photochemical processing are interpreted from long-term trends in ozone and NO_x oxidation products.

2. Methods

2.1. Data Sets

[7] Data for this analysis are compiled from measurements performed in the SoCAB between 1960 and 2010.

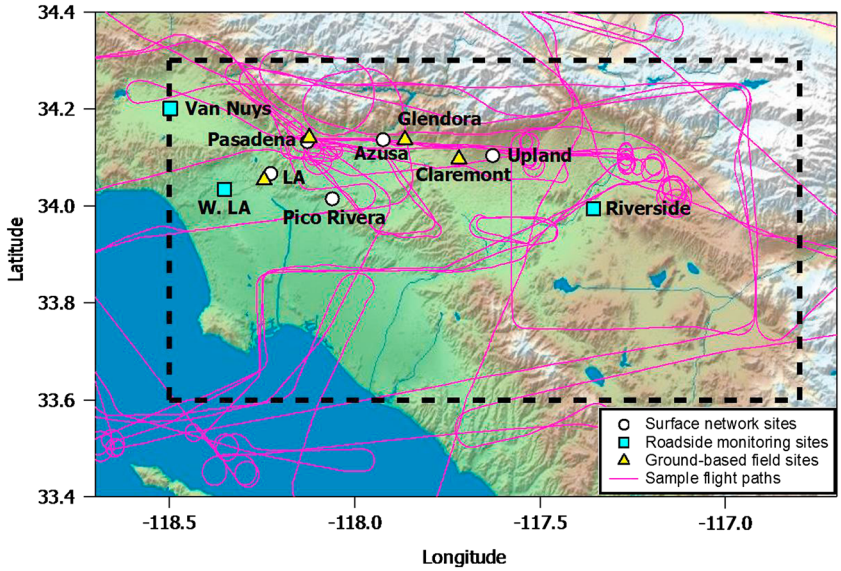

Figure 2. Measurements for this analysis are compiled from surface network sites (white circles), roadside monitors (cyan squares), ground-based field sites (yellow triangles), and airborne studies (sample flight tracks in pink). Airborne measurements collected in the mixed boundary layer (<1 km) over the SoCAB (dashed box) are interpreted as basin-wide averages.

Measurements are acquired from (1) the South Coast Air Quality Monitoring District (SCAQMD) and Photochemical Assessment Monitoring Stations (PAMS) surface network, (2) mobile roadside monitors, (3) ground-based field studies, and (4) chemically instrumented research aircraft. Figure 2 illustrates the locations of the network monitoring sites and ground-based field study locations as well as example flight tracks from the airborne experiments used in this analysis.

2.1.1. Surface Network Stations

[8] Trace gas data since the 1970s were acquired from the web-based Air Quality Data Statistics database maintained by the California Air Resources Board (CARB) (http://www.arb.ca.gov/adam/index.html) for select monitoring stations in the SoCAB network. These data include annual 8 h maximum ozone concentrations; hourly measurements of NO, NO_2, and CO; and 3 h canister samples of volatile organic compounds (VOCs). We focus on data collected from the Azusa and Upland sites due to their long-term data coverage and proximity to ground-based field study locations; data coverage and measurement techniques at these stations are summarized in Table 1. We use the available NO_2 data from these ground sites despite a known sensitivity of the NO_2 measurements to organic nitrates and HNO_3, which depends upon inlet configuration and thermal operation range of a molybdenum converter [*Fehsenfeld et al.*, 1990; *Fitz*, 2002; *Murphy et al.*, 2007; *Winer et al.*, 1974]. NO_x mixing ratios are calculated as the sum of the reported NO and NO_2 measurements. Since precursors in the SoCAB primarily arise from motor vehicle emissions, we focus our analysis on VOC species characteristic of automobile exhaust, including benzene,

Table 1. Summary of Trace Gas Data From the Azusa and Upland Network Stations in the SoCAB

Measurement	Site	Data Coverage	Technique[a]
VOC[b]	Azusa	1974–1975, 1995–2010	Canister collection followed by gas chromatography
	Upland	1975, 1994–2008	Canister collection followed by gas chromatography
O_3	Azusa	1978–2010	Ultraviolet absorption
	Upland	1975–2010	Ultraviolet absorption
CO	Azusa	1975–2010	Nondispersive infrared absorption
	Upland	1975–2010	Nondispersive infrared absorption
NO	Azusa	1975–1979	Colorimetry
	Azusa	1980–2010	Ozone-induced chemiluminescence
	Upland	1975–2010	Ozone- induced chemiluminescence
NO_2[c]	Azusa	1975–1979	Colorimetry using Lyshkow-modified Saltzman reagent
	Azusa	1980–2010	Heated molybdenum converter followed by chemiluminescence
	Upland	1975–2010	Heated molybdenum converter followed by chemiluminescence

[a]Additional information about measurement techniques and instrumentation are available on the CARB website (http://www.arb.ca.gov/airwebmanual/index.php).

[b]VOC measurements (non-methane organic carbon (NMOC) in the original data files) represent 3 h samples collected on a varying schedule during a 3 month period from July through September. Years represent data coverage for benzene, toluene, ethylbenzene, and *o*-xylene; measurements of isoprene are only available at Azusa and Upland between 1994 and 2008.

[c]NO_2 measurements since 1980 at Azusa and 1975 at Upland include a known sensitivity to organic nitrates and HNO_3, which depends upon inlet configuration and thermal operation range of the molybdenum converter [*Fehsenfeld et al.*, 1990; *Fitz*, 2002; *Murphy et al.*, 2007; *Winer et al.*, 1974]; NO_x is calculated as the sum of the NO and NO_2 measurements.

Table 2. Summary of Roadside Measurements in the SoCAB

Year	Dates	Location	Reference
1991	19 May to 27 Jun	Los Angeles	*Beaton et al*. [1995]
1999	15 Oct to 19 Oct	Los Angeles	*Bishop and Stedman* [2008]
	28 Jun to 7 Jul	Riverside	
2000	30 May to 6 Jun	Riverside	*Bishop and Stedman* [2008]
2001	15 Oct to 19 Oct	Los Angeles	*Bishop and Stedman* [2008]
	6 Jun to 13 Jun	Riverside	
2003	27 Oct to 31 Oct	Los Angeles	*Bishop and Stedman* [2008]
2005	17 Oct to 21 Oct	Los Angeles	*Bishop and Stedman* [2008]
2008	17 Mar to 21 Mar	Los Angeles	*Bishop et al*. [2010]; *Stedman et al*. [2009]
2010	12 Aug to 16 Aug	Van Nuys	*Bishop et al*. [2012]

toluene, ethylbenzene, and *o*-xylene. Measurements of isoprene are used to assess potential changes in biogenic emissions over time. Although network measurements of VOCs (also called non-methane organic compounds (NMOCs) in the data sets) date as far back as 1990 [*Warneke et al*., 2012], we only utilize quality-reviewed data since 1994 for this analysis. Network measurements of VOCs below the instrumental limit of detection are reported by CARB as one-half the limit of detection. Measurements of VOCs are converted from units of parts per billion of carbon (ppbC) to parts per billion by volume (ppbv) of compound prior to further analysis.

2.1.2. Roadside Monitors

[9] Ozone precursor emissions from light-duty and heavy-duty vehicles measured by mobile roadside monitors in California are available from peer-reviewed publications [*Bishop and Stedman*, 2008; *Bishop et al*., 2010; *Bishop et al*., 2012; *Stedman et al*., 2009] and research reports accessible from the Fuel Efficiency Automobile Test (FEAT) website (http://www.feat.biochem.du.edu). We use measurements of NO, CO, and total unspeciated hydrocarbons (total HC) including methane from light-duty vehicles acquired at the Los Angeles, Van Nuys, and Riverside monitoring sites since 1991 [*Bishop and Stedman*, 2008; *Bishop et al*., 2010]; measurement periods and locations are summarized in Table 2. For this analysis, we assume that NO_x is primarily emitted as NO [*Soltic and Weilenmann*, 2003] and that there is negligible chemical processing between emission and detection given the sampling configuration of the instrument [*Burgard et al*., 2006]; roadside measurements of NO are thus referred to as NO_x in the following analysis. Molar emission ratios of CO, NO_x, and (total HC) to CO_2 are derived from the reported fuel-specific emissions of grams of pollutant per kilogram of fuel [*Bishop and Stedman*, 2008; *Burgard et al*., 2006; *Singer et al*., 1998].

2.1.3. Ground-Based and Airborne Field Studies

[10] The SoCAB has been the focus of many ground-based and airborne air quality field campaigns. Compound-specific VOCs, NO_x, and CO and secondary oxidation products such as O_3, PAN, and HNO_3 have been measured during these studies. The species measured, measurement techniques, data coverage, sampling locations, and references for field studies performed between 1960 and 2010 are summarized in Table 3.

[11] Our historical analysis of precursor emissions begins with ground-based measurements of VOCs and NO_x in downtown Los Angeles in 1960 by *Neligan* [1962]. This study was followed with additional measurements by the California Air Pollution Control District in 1963 [*Leonard et al*., 1976], *Lonneman et al*. [1968] in 1966, *Altshuller et al*. [1971] in 1967, and *Kopczynski et al*. [1972] in 1968. Data from these studies were acquired from tables and text within the cited literature.

[12] More extensive ground-based field studies supported by CARB and SCAQMD began in 1987 with the Southern California Air Quality Study (SCAQS) and continued with the Los Angeles Atmospheric Free Radical Study (LAAFRS) in 1993 and the Southern California Ozone Study (SCOS) in 1997. SCOS 1997 incorporated measurements from several instrumented aircraft, although we use measurements only from the Piper Aztec aircraft due to its primary sampling objective to characterize ozone and precursors in the SoCAB [*Croes and Fujita*, 2003]. Archived data from field projects supported by CARB were acquired directly from CARB. Peer-reviewed publications outlining objectives, measured species, measurement techniques, sampling details, and results are available for most field studies; research reports are available for the remainder on the CARB website (http://www.arb.ca.gov/research/research.htm).

[13] Airborne measurements are also compiled from several field campaigns performed in the SoCAB in the past decade. A chemically instrumented NOAA P-3 aircraft sampled the daytime mixed layer throughout the Los Angeles Basin on 13 May 2002 during the Intercontinental Transport and Chemical Transformation (ITCT) study [*Parrish et al*., 2004], and the NASA DC-8 aircraft sampled the same general area on 18 June 2008 during the California phase of the Arctic Research of the Composition of the Troposphere from Aircraft and Satellites study (ARCTAS-CARB) [*Jacob et al*., 2010]. Most recently, the California Research at the Nexus of Air Quality and Climate Change (CalNex) field project in May, June, and July 2010 reported chemical measurements in the Los Angeles mixed layer from the NOAA P-3 aircraft and from a ground site in Pasadena, California [*Ryerson et al*., 2013]. Archived data for the field studies conducted by NOAA and NASA are publicly available on each institution's website (http://www.esrl.noaa.gov/csd/field.html; http://www-air.larc.nasa.gov/missions.htm).

[14] Airborne and ground-based measurements of secondary oxidation products, such as PAN and HNO_3, are available from SCAQS 1987, SCOS 1997, ITCT 2002, ARCTAS-CARB 2008, and CalNex 2010. Additional measurements are reported in the literature for ground-based field studies near Riverside in 1962 [*Darley et al*., 1963] and 1982 [*Russell et al*., 1988a]; Los Angeles in 1968 [*Kopczynski et al*., 1972]; Pasadena in 1973 [*Hanst et al*., 1982]; West Covina in 1973 by *Spicer* [1977b]; Claremont in 1978 by *Tuazon et al*. [1981] and 1985 by *Grosjean* [1986, 1988]; Glendora in 1986 by *Anlauf et al*. [1991]; and Tanbark Flats in 1990 and 1991 by *Grosjean et al*. [1993].

[15] Ground-based field measurements of hydrogen peroxide (H_2O_2) are available from the Carbonaceous Species Methods Comparison Study (CSMCS) at Glendora in 1986 [*Kok et al*., 1990; *Mackay et al*., 1990; *Sakugawa and*

Table 3. Summary of Measurements From Airborne and Ground-Based Field Studies in the SoCAB

Year	Dates	Location	Measurement	Technique	References
1960	18 Aug to 18 Nov	Los Angeles	NO_x, CO[i]	Nearby monitoring station	*Neligan* [1962]
			Benzene, toluene[i]	Gas chromatography	
			PAN[j]	Polyethylene bag collection followed by long-path Fourier transform infrared spectroscopy	*Renzetti and Bryan* [1961]
1962	N/A	Riverside	PAN[j]	Electron capture-gas chromatography	*Darley et al*. [1963]
1963–1965	20 Apr to 6 Nov	Los Angeles	Benzene, toluene[j]	Gas chromatography	*Leonard et al*. [1976]
1966	1 Sep to 30 Nov	Pasadena/ Los Angeles	NO_x, CO[j]	Nearby monitoring station	*Lonneman et al*. [1968]
			Toluene, ethylbenzene, *o*-xylene[j]	Tedlar bag collection followed by gas chromatography	
1967	19 Sep to 17 Nov	Los Angeles/ Azusa	Toluene, ethylbenzene, *o*-xylene[j]	Tedlar bag collection followed by gas chromatography	*Altshuller et al*. [1971]
1968	5 Sep to 13 Nov	Los Angeles	NO_x[j]	Chromium trioxide paper and Griess-Saltzman reagent	*Kopczynski et al*. [1972]; *Lonneman et al*. [1976]
			Toluene, ethylbenzene, *o*-xylene, CO[j]	Tedlar bag collection followed by gas chromatography	
			PAN[j]	Gas chromatography-electron capture detection	*Lonneman et al*. [1976]
1970	7, 10 Aug	Riverside	H_2O_2[j]	Teflon bag collection followed by colorimetry with Ti (IV)	*Bufalini et al*. [1972]
1971	23 Aug to 14 Oct	Los Angeles	Benzene, toluene[j]	Gas chromatography	*Leonard et al*. [1976]
1973	2 Jul to 30 Aug	Los Angeles	Benzene, toluene[j]	Gas chromatography	*Leonard et al*. [1976]
1973	24 Jul to 26 Jul	Pasadena	PAN[i]	Long-path Fourier transform infrared spectroscopy	*Hanst et al*. [1975]
1973	24 Aug to 28 Sep	West Covina	O_3, NO, NO_x[i]	Chemiluminescence	*Spicer* [1977a]; *Spicer* [1977b]
			PAN[i]	Gas chromatography-electron capture detection	
			HNO_3[i]	Acid-detecting mast colorimetry	
1977	19 Jul to 29 Jul	Claremont/ Riverside	H_2O_2[j]	Scrubbing coil impinger followed by luminol-based chemiluminescence	*Kok et al*. [1978]
1978	9 Oct to 13 Oct	Claremont	NO, NO_2[i]	Chemiluminescence	*Tuazon et al*. [1981]
			O_3, PAN, HNO_3[i]	Long-path Fourier transform infrared spectroscopy	
1979	9 Apr to 21 Apr	Los Angeles	Benzene, toluene, ethylbenzene, *o*-xylene[j]	Canister/Gas Chromatography-flame ionization detector	*Singh et al*. [1981]
			PAN[j]	Gas chromatography-electron capture detection	
1980	26 Jun to 27 Jun	Los Angeles	CO, NO, NO_2, NO_x, PAN, HNO_3, O_3[i]	Long-path Fourier transform infrared spectroscopy	*Hanst et al*. [1982]
1982	31 Aug	Pasadena/ Riverside	PAN[j]	Gas chromatography-electron capture detection	*Russell et al*. [1988a]
1985[a]	11 Sep to 18 Sep	Claremont	O_3	UV absorption (from nearby monitoring station)	
			NO, NO_2[i]	Chemiluminescence	*Grosjean* [1988]
			PAN[i]	Gas chromatography-electron capture detection	
			HNO_3[i]	Filter pack followed by ion chromatography; Fourier transform infrared spectroscopy	*Winer et al*. [1986]
1986[b]	12 Aug to 21 Aug	Glendora	HNO_3[j]	Fourier transform infrared spectroscopy; Tunable diode laser absorption spectroscopy; Filter pack followed by ion chromatography	*Anlauf et al*. [1991]
			H_2O_2[j]	Dual coil impinger followed by dual enzyme fluorescence;	*Kok et al*. [1990]
				Impinger with diffusion scrubber followed by dual enzyme fluorescence;	*Tanner and Shen* [1990]
				Cryogenic trap followed by dual enzyme fluorescence;	*Sakugawa and Kaplan* [1990]
				Tunable diode laser absorption spectroscopy	*Mackay et al*. [1990]
1987[c]	19 June to 3 Sep	Claremont	O_3, NO_x, NO_y[k]	Chemiluminescence	*Fujita et al*. [1992]; *Lawson* [1990]; *Williams and Grosjean* [1990]
			PAN[k]	Gas chromatography-electron capture detection	*Williams and Grosjean* [1990]
			HNO_3[k]	Tunable diode laser absorption spectroscopy	
			CO, benzene, toluene, *o*-xylene, isoprene[k]	Canister/Gas Chromatography-flame ionization detector	
			H_2O_2[j]	Tunable diode laser absorption spectroscopy	*Mackay et al*. [1988]
1990	3 Aug to 5 Sep	Tanbark Flat	PAN[j]	Gas chromatography-electron capture detection	*Grosjean et al*. [1993]
1991	5 Aug to 12 Sep	Tanbark Flat	PAN[j]	Gas chromatography-electron capture detection	*Grosjean et al*. [1993]
1993[d]	1 Sep to 26 Sep	Claremont	O_3[k]	UV absorption	*Mackay* [1994]
			NO_2, NO_x, NO_y[k]	Chemiluminescence	
			CO, benzene[k]	Canister and DNPH cartridge followed by gas chromatography-flame ionization detector	
			PAN[k]	Gas chromatography/chemiluminescence	
			HNO_3, H_2O_2[k]	Tunable diode laser absorption spectroscopy	

Table 3. (continued)

Year	Dates	Location	Measurement	Technique	References
1997[e]	16 Jun to 15 Oct	Azusa	O_3[k]	UV absorption	*Blumenthal* [1999]; *Croes and Fujita* [2003]; *Fitz* [1999]; *Fujita et al.* [1999]; *Grosjean* [2003]; *Grosjean et al.* [2001]
			NO_y[k]	Chemiluminescence	
			CO, CO_2, benzene, toluene, ethylbenzene, *o*-xylene[k]	Canister and DNPH cartridge followed by gas chromatography-flame ionization detection	
			PAN[k]	Gas chromatography-electron capture detection	
			HNO_3[k]	Tunable diode laser absorption spectroscopy	
1997[e]	16 Jun to 15 Oct	Piper Aztec aircraft	O_3[k]	UV absorption	*Croes and Fujita* [2003]; *Fitz* [1999]; *Fujita et al.* [1999]; *Grosjean* [2003]; *Grosjean et al.* [2001]
			NO_y[k]	Chemiluminescence	
			CO, CO_2, benzene, toluene, *o*-xylene[k]	Canister and DNPH cartridge followed by gas chromatography-flame ionization detection	
2002[f]	13 May	NOAA P-3 aircraft	O_3, NO_x, NO_y[l]	Chemiluminescence	*Parrish et al.* [2004]
			CO[l]	Vacuum UV resonance fluorescence	
			CO_2[l]	Nondispersive infrared absorption	
			PAN, HNO_3[l]	Chemical ionization mass spectrometry	
			benzene, toluene, *o*-xylene[l]	Whole air sampler followed by gas chromatography	
2008[g]	13 May	NASA DC-8 aircraft	O_3, NO_x, NO_y[m]	Chemiluminescence	*Jacob et al.* [2010]
			CO[m]	Vacuum UV resonance fluorescence	
			CO_2[m]	Nondispersive infrared absorption	
			PAN, HNO_3[m]	Chemical ionization mass spectrometry	
			benzene, toluene[m]	Proton transfer reaction mass spectrometry	
2010[h]	1 May to 30 Jun	NOAA P-3 aircraft	O_3, NO_x, NO_y[l]	Chemiluminescence	*Ryerson et al.* [2013]
			CO[l]	Vacuum UV resonance fluorescence	
			CO_2[l]	Wavelength-scanned cavity ring-down spectroscopy	
			PAN, HNO_3[l]	Chemical ionization mass spectrometry	
			benzene, toluene, ethylbenzene, *o*-xylene[l]	Whole air sampler followed by gas chromatography	
2010[h]	15 May to 15 Jun	Pasadena	O_3[l]	UV absorption	*Ryerson et al.* [2013]
			NO_x, NO_y[l]	Chemiluminescence	
			CO[l]	Vacuum UV resonance fluorescence	
			CO_2[l]	Nondispersive infrared absorption	
			PAN, HNO_3[l]	Chemical ionization mass spectrometry	
			benzene, toluene, ethylbenzene, *o*-xylene[l]	Gas chromatography-mass spectrometry	

[a]Nitrogen Species Methods Comparison Study (NSMCS) 1985.
[b]Carbonaceous Species Methods Comparison Study (CSMCS) 1986.
[c]Southern California Air Quality Study (SCAQS) 1987.
[d]Los Angeles Atmospheric Free Radical Study (LAAFRS) 1993.
[e]Southern California Ozone Study (SCOS) 1997.
[f]Intercontinental Transport and Chemical Transformation (ITCT) 2002.
[g]CARB phase of Arctic Research of the Composition of the Troposphere from Aircraft and Satellites (ARCTAS-CARB) 2008.
[h]California Research at the Nexus of Air Quality and Climate Change (CalNex) 2010.
[i]Data reported in the cited literature.
[j]Average values reported in the literature reference.
[k]Data requested from CARB.
[l]Data acquired from NOAA website (http://www.esrl.noaa.gov/csd/field.html).
[m]Data acquired from NASA website (http://www-air.larc.nasa.gov/missions.htm).

Kaplan, 1990; *Tanner and Shen*, 1990], SCAQS 1987 [*Mackay*, 1988], and LAAFRS 1993 [*Mackay*, 1994]; airborne measurements of H_2O_2 are available from ARCTAS-CARB 2008 [*Jacob et al.*, 2010]. Hourly measurements of H_2O_2 were obtained upon request from CARB for LAAFRS, and 15 s H_2O_2 data were acquired from the NASA website for ARCTAS-CARB. All other data points represent reported averages or maxima from the literature. Historical measurements of H_2O_2 are summarized in Table 3. Earlier reports of H_2O_2 dating back to 1970 at Riverside [*Bufalini et al.*, 1972] and 1977 at Claremont [*Kok et al.*, 1978] were later invalidated owing to an interference of the H_2O_2 collecting solution with ozone and possible aqueous reactions of H_2O_2 with other gases [*Kok et al.*, 1988; *Lee et al.*, 2000]. Eliminating the data points from 1970 and 1977 leaves too few measurements to identify a significant trend; thus, further interpretation of H_2O_2 data in the SoCAB is not attempted here.

[16] A historical account of alkyl nitrates is also not reported here owing to a lack of field measurements. For analyses requiring total reactive nitrogen (NO_y) in section 4.3, we assume alkyl nitrates are a relatively small contribution to the sum of reactive nitrogen species in the Los Angeles basin. We support this assumption by comparing daytime measurements of gas-phase NO_y with the calculated sum of NO_y, where $\Sigma NO_y = NO_x + PAN + HNO_3$ [*Parrish et al.*, 1993], from four field studies between 2002 and 2010. Quantitative

Table 4. Rate of Change (Δ) and Corresponding 1σ Standard Deviation in Units of Percent Change Per Year for Abundances and Emissions Ratios of Ozone and Its Precursors[a]

	Field Observations[b]			Roadside Monitors			AQMD Network—Azusa			AQMD Network—Upland			All Observations[c]		
Measurement	Δ (% yr^{-1})	r^2	N	Δ (% yr^{-1})	r^2	N	Δ (% yr^{-1})	r^2	N	Δ (% yr^{-1})	r^2	N	Δ (% yr^{-1})	r^2	N
O_3 (8 h max)							-3.4 ± 0.2	0.88	33	-3.0 ± 0.1	0.92	38	-2.8 ± 0.1[d]	0.91	38
NO_x	-5.2 ± 1.0	0.82	8				-2.0 ± 0.3	0.68	21	-1.8 ± 0.3	0.51	36	-2.6 ± 0.3	0.56	65
CO	-7.9 ± 0.8	0.95	7				-4.8 ± 0.4	0.89	21	-5.2 ± 0.4	0.87	26	-5.7 ± 0.3	0.86	54
Benzene	-8.6 ± 0.8	0.94	9				-7.4 ± 0.5	0.94	17	-7.6 ± 0.8	0.88	15	-8.0 ± 0.3	0.94	41
Toluene	-8.0 ± 0.8	0.91	11				-6.6 ± 0.4	0.95	17	-5.7 ± 0.6	0.86	16	-6.7 ± 0.3	0.92	44
Ethylbenzene	-8.6 ± 0.9	0.95	6				-5.8 ± 0.6	0.85	17	-4.2 ± 1.0	0.55	16	-6.9 ± 0.4	0.87	39
o-Xylene	-8.7 ± 1.0	0.94	7				-8.5 ± 0.6	0.93	17	-6.7 ± 0.7	0.87	16	-7.5 ± 0.3	0.93	40
Isoprene							0.7 ± 2.1	0.01	14	0.3 ± 0.9	0.01	15			
CO/CO_2	-11.6 ± 1.7	0.92	6	-9.9 ± 1.0	0.92	10							-11.5 ± 1.4[e]	0.82	16
NO_x/CO_2[f]	-5.5 ± 2.6	0.52	6	-7.0 ± 1.0	0.86	9							-6.6 ± 1.7[e]	0.52	15
(Total HC)/CO_2				-11.6 ± 1.0	0.83	10									
Benzene/CO_2	-7.7 ± 1.3	0.88	6												
NO_x/CO[f]	5.2 ± 1.4	0.59	12	5.9 ± 1.3	0.77	9	3.6 ± 0.7	0.68	17	5.5 ± 0.4	0.89	26	4.9 ± 0.4	0.71	67
(Total HC)/CO				-1.8 ± 2.3	0.07	10									
Benzene/CO	-1.1 ± 0.6	0.30	10				0.7 ± 0.6	0.08	17	-1.6 ± 0.4	0.70	8	-1.2 ± 0.4	0.20	35
(Total HC)/NO_x				-2.0 ± 2.7	0.08	9									
Toluene/NO_x	-4.4 ± 0.7	0.86	9				-3.8 ± 0.7	0.68	17	-5.1 ± 0.9	0.69	16	-4.6 ± 0.4	0.78	42
Ethylbenzene/NO_x	-4.5 ± 0.4	0.97	5				-3.0 ± 0.9	0.44	17	-5.9 ± 2.0	0.40	15	-4.2 ± 0.6	0.60	37
o-Xylene/NO_x	-5.6 ± 0.7	0.92	7				-5.5 ± 0.7	0.80	17	-5.4 ± 1.8	0.40	15	-5.7 ± 0.5	0.77	39

[a]A negative rate of change signifies a decreasing trend over time; N represents the number of data points, corresponding to years of data, used for linear regression.
[b]Overall trend since 1960 for ground-based observations of precursor abundances, overall trend since 1960 for airborne and ground-based observations of precursor emissions ratios.
[c]Overall trend since 1960 representing combined data from the available field, roadside, and network observations.
[d]Overall trend since 1973 determined from maximum 8 h average ozone for all sites in the SoCAB (Figure 1).
[e]Overall trend since 1991 representing a combined LLS fit of the available field and roadside observations.
[f]NO_y used for emissions ratios from airborne and ground-based field studies where available.

agreement within 1σ uncertainties, which typically range from ±10% to ±20% of the mixing ratio, between measured NO_y and ΣNO_y suggests little contribution on average from other species to NO_y during the most recent decade of our long-term analysis. An earlier account of alkyl nitrate contributions in the SoCAB reported by *Grosjean* [1983] showed mixing ratios of methyl nitrate up to ~5 ppbv during photochemical smog episodes in Claremont in 1980; however, methyl nitrate contributed <5% to ΣNO_y since NO_x, PAN, and HNO_3 were also significantly enhanced during this time period.

[17] Accuracy of the utilized data is considered in this analysis. For data sets found in the literature, we assume that measurements were subjected to quality analysis and peer review prior to publication and that any concerns with data quality, measurement technique, instrumentation, or sampling were reported with the published data or in subsequent publications. For field study data provided by CARB, we assume that final reported data have been subjected to quality analysis with questionable data points eliminated or flagged appropriately. Where available, information regarding measurement uncertainties, precision, and possible interferences by other species is taken from data file headers and supporting documents.

2.2. Data Analysis

[18] This analysis is focused on measurements during summertime, when ozone production is at a maximum, and weekdays, when precursor emissions are most prominent. Surface network measurements are limited to data collected between 1 May and 30 September; field study data are averaged over the collection periods summarized in Table 3, which take place between May and November and range from a single day to several months. With the exception of the aircraft campaigns where flight times are typically during midday, measurements of VOCs, CO, and NO_x are further limited to samples collected on weekday mornings between 0500 and 0900 PDT when precursor emissions are at a maximum and prior to development of a well-mixed planetary boundary layer and extensive photochemical processing. Conversely, measurements of oxidation products, including O_3, PAN, and HNO_3, are taken from weekday afternoons between 1200 and 1800 PDT when the planetary boundary layer is well developed and accumulated concentrations of secondary pollutants are at a maximum.

[19] To simplify the analysis, we group the available ground-based measurements from various locations throughout the SoCAB into two general geographic areas. The first includes sampling sites on the western side of the SoCAB located near major centers of emissions, such as Los Angeles, Pasadena, Azusa, and Glendora, and the second includes locations generally downwind, such as Upland, Claremont, and Riverside, on the eastern side of the basin. We distinguish data points acquired from the two defined areas for comparison. Airborne measurements from the mixed boundary layer over the SoCAB between 0.2 and 1 km above ground level, $33.6° < \text{latitude} < 34.3°$, and $-118.5° < \text{longitude} < -116.8°$ [*Pollack et al.*, 2012], are retained for this analysis as a representative of basin-wide averages.

[20] Previously reported values for average atmospheric abundances and emissions ratios of ozone precursors and secondary pollutants are taken from the literature where available. Otherwise, we calculate average abundances and emissions ratios from the data sets described above.

Table 5. Rate of Change (Δ) and Corresponding 1σ Standard Deviation in Units of Percent Change per Year for Abundances and Emission Ratios of Precursors From the EMFAC2011 Emission Inventory Between 1990 and 2010 [*CARB*, 2011, Accessed January 2013] and the CARB Emission Inventory for the SoCAB Between 1975 and 2010 [*CARB*, 2009, Accessed January 2013][a]

	EMFAC2011-LDV			EMFAC2011-SG			CARB Inventory			CARB Inventory		
	(Light-Duty Gasoline Vehicles)			(Light-Duty Gasoline + Heavy-Duty Diesel)			(On-Road Sources)			(All Sources)		
Measurement	Δ (% yr^{-1})	r^2	N	Δ (% yr^{-1})	r^2	N	Δ (% yr^{-1})	r^2	N	Δ (% yr^{-1})	r^2	N
NO_x	-6.2 ± 0.3	0.99	5	-4.2 ± 0.7	0.91	5	-2.2 ± 0.5[b]	0.85	8	-2.1 ± 0.4[b]	0.85	8
ROG	-8.4 ± 0.2	1.00	5	-8.2 ± 0.2	1.00	5	-6.2 ± 0.4[b]	0.96	8	-4.4 ± 0.4[b]	0.96	8
CO	-8.5 ± 0.2	1.00	5	-8.4 ± 0.1	1.00	5	-5.8 ± 0.5[b]	0.96	8	-4.9 ± 0.4[b]	0.96	8
CO_2	1.5 ± 0.1	0.98	5	1.6 ± 0.2	0.96	5	0.4 ± 0.1[c]	0.74	20	0.9 ± 0.1[c]	0.74	20
CO/CO_2	-9.9 ± 0.3	1.00	5	-9.8 ± 0.3	1.00	5						
NO_x/CO_2	-7.6 ± 0.3	0.99	5	-5.6 ± 0.6	0.96	5						
ROG/CO_2	-9.6 ± 0.3	1.00	5	-9.6 ± 0.3	1.00	5						
NO_x/CO	2.5 ± 0.3	0.96	5	4.6 ± 0.9	0.90	5	3.7 ± 0.2	0.99	8	2.9 ± 0.2	0.99	8
ROG/CO	0.1 ± 0.1	0.20	5	0.2 ± 0.1	0.43	5	-0.5 ± 0.1	0.62	8	0.5 ± 0.1	0.74	8
ROG/NO_x	-2.4 ± 0.4	0.92	5	-4.2 ± 0.9	0.87	5	-4.1 ± 0.2	0.99	8	-2.3 ± 0.2	0.97	8

[a]A negative rate of change signifies a decreasing trend over time; N represents the number of data points used for linear regression.
[b]NO_x, ROG, and CO from all emissions sources in the SoCAB [*CARB*, 2008a, accessed January 2013].
[c]Gross CO_2 emissions from the statewide greenhouse gas inventory [*CARB*, 2008a, accessed January 2013].

Average abundances are calculated as the arithmetic mean of all retained measurements for a given substance during the specified collection periods. The corresponding uncertainties represent a confidence limit calculated by dividing the 1σ standard deviation of the mean by the square root of the number of days of observations. Emissions ratios of directly emitted species, and enhancement ratios involving secondary oxidation products, are determined by linear least squares (LLS) [*Press et al*., 1988] orthogonal distance regression (ODR) [*Boggs et al*., 1987] to the relevant observations; the slope of the fitted line is interpreted as the emissions or enhancement ratio [*Pollack et al*., 2012]. Where information is available, the LLS ODR fits are weighted by the imprecision of the measurements, and a total uncertainty for each ratio is calculated by quadrature additions of the uncertainty in the fitted slope and the uncertainties of the respective measurements [*Taylor*, 1997]. Error bars associated with these ratios reflect measurement uncertainty as well as day-to-day variability. For data sets where instrument accuracy and precision information are not reported, uncertainty in the emissions ratio is reported as the 1σ standard deviation of the slope.

[21] LLS regression analysis of the logarithmic-transformed data is used to quantify the exponential change describing the trends in abundances and emissions ratios of ozone precursors (Table 4) as well as abundances and enhancement ratios of secondary oxidation products (Table 6). Extracting information about the trends from a functional fit to multiyear data minimizes the influence of interannual variability from various measurement sites, platforms, meteorological conditions, and possible pollution episodes. Here long-term changes are quantified and reported in two ways: (1) a constant rate of change, R, reported in units of percent change per year, and (2) a factor of change, f, spanning the range of years of available measurements. We assume an exponential function (1) for changes in abundances and emissions ratios over time.

$$y_t = y_0 \times e^{-at} \tag{1}$$

[22] Rates and factors of change for a given species, y, are then derived from the slope, a, derived from a LLS fit to the logarithmic-transformed data points, as described by equations (2)–(5):

$$\ln(y_0) - \ln(y_t) = a \times t \tag{2}$$

$$\Delta \ln(y) = a, \quad \text{for } \Delta t = 1 \text{ year} \tag{3}$$

$$R = \Delta(y) = e^a \times 100, \quad \text{for } \Delta t = 1 \text{ year} \tag{4}$$

$$f = \frac{y_0}{y_t} = (e^{-a})^t \tag{5}$$

[23] The R percent change per year ($\Delta t = 1$ year) is determined from (4), and the f factor of change over the full time period of the historical measurements (e.g., $\Delta t = 50$ years for measurements between 1960 and 2010) is determined from (5). The LLS fits are not weighted by the uncertainties of the individual data points due to differences in calculating the reported uncertainties for abundances and emissions ratios described above. Uncertainties associated with the rate and factor of change reflect propagation of the 1σ standard deviation of the fitted slope.

[24] This analysis method is also used to determine trends in emissions and emission ratios of precursors in bottom-up emission inventories. Annual average emissions predicted by the inventories are typically reported by mass in units of short tons d^{-1}, except for CO_2 from the CARB greenhouse gas inventory which is reported in metric tons d^{-1}. Molar emission ratios are calculated from annual average mass emissions by converting to metric tons then dividing by molecular weight (i.e., 0.028 kg/mol for CO, 0.046 kg/mol for NO_2, and 0.044 kg/mol for CO_2). Emissions and emission ratios involving unspeciated reactive organic gases (ROG) are not converted to molar values but are instead reported on an arbitrary scale. In sections 3.1 and 3.2, we compare trends in ambient measurements using airborne and ground-based field studies and surface network observations to inventory emission trends estimated by summing all source contributions in the yearly CARB emission inventories for the SoCAB [*California Air Resources Board* (*CARB*), 2009, accessed

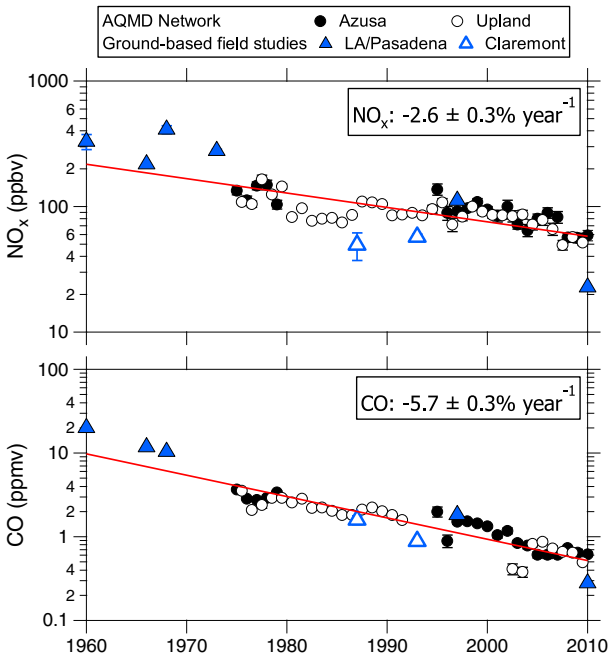

Figure 3. Average abundances of NO_x (in units of ppbv) and CO (in units of ppmv) measured at the Azusa (solid black circles) and Upland (open circles, offset by 0.5 years on x axis) surface network sites and ground-based field campaigns near LA/Pasadena (solid blue triangles) and Claremont (open blue triangles) since 1960. Error bars represent confidence limits based on the number of days of observations per year. LLS fits (red lines) represent long-term trends in NO_x and CO abundances.

January 2013]. In section 3.2, we specifically compare trends in near-tailpipe measurements of light-duty gasoline-fueled vehicles (LDV) from roadside monitors to the EMFAC2011 on-road mobile emission inventory for this subset of vehicles (Table 5) [*CARB*, 2011, accessed January 2013].

[25] In section 4, trends in secondary oxidation products determined from ambient measurements are compared with simulated mixing ratios [*Fujita et al.*, 2013] predicted using a chemical box model.

3. Trends in Ozone and Its Precursors

3.1. Atmospheric Abundances

[26] Figure 1 illustrates the significant decrease in ozone concentrations observed in the SoCAB since the 1970s. The data points represent maximum 8 h average ozone mixing ratios measured basin wide and at selected individual surface monitoring network stations in the SoCAB for a 1 year period. Basin-wide measurements represent the maximum value reported from any of the individual network sites in the SoCAB in a given year, while selected individual sites are depicted to demonstrate the progression of ozone from coastal to inland sites across the basin. Here we derive the factor and rate of change in ozone from the slope of the LLS regression of the natural log of the basin-wide maximum 8 h ozone values in Figure 1. The data show that ozone maximum concentrations in the SoCAB have decreased at a rate of $2.8 \pm 0.2\%\,yr^{-1}$, equivalent to a decrease of a factor of 2.9 over nearly four decades. Although the maximum 8 h average ozone from the individual sites is often less than the basin-wide average, LLS fits of the long-term trends from the individual sites show similar rates of decrease in ozone (average of $3.3 \pm 0.2\%\,yr^{-1}$ for the five sites shown in Figure 1). We find that the basin-wide data are well fit by a constant exponential decrease of $2.8\%\,yr^{-1}$ with no indication of a change in that rate between 1973 and 2010, in contrast to recent descriptions of ozone trends [e.g., *Fujita et al.*, 2013; *Warneke et al.*, 2012] that have invoked a slower rate of decrease in ozone in Los Angeles after 1999. Inclusion of a constant term in the fitting expression to represent a nonnegligible ozone background does not significantly improve the residuals to the data points in Figure 1. However, the constant rate of change must slow when future ozone concentrations approach baseline ozone levels transported into the SoCAB.

[27] The observed trend in ozone is positively correlated with trends in its precursors. Time series plots of the annually averaged abundances of NO_x and CO (Figure 3) and select VOCs (Figure 4) using data from the literature, ground-based field campaigns, and the Azusa and Upland SCAQMD surface network stations demonstrate large decreases in precursor emissions over the past five decades [*McDonald et al.*, 2012; *Warneke et al.*, 2012]. Considering all data, abundances of NO_x have decreased at an average rate of $2.6 \pm 0.3\%\,yr^{-1}$, resulting in a factor of 3.7 decrease over the 50 years between 1960 and 2010. There are site-specific differences in the observed rates, but we take the combined observations from all locations as the most robust indication of the rate of NO_x decrease in the SoCAB. The combined rate of decrease reported here of $2.6 \pm 0.3\%\,yr^{-1}$ is in agreement with NO_x emissions trends in the CARB emissions inventory [*CARB*, 2009, accessed January 2013], which predict an annual average decrease in NO_x of $2.1 \pm 0.4\%\,yr^{-1}$ for all sources between 1975 and 2010 (Table 5).

[28] Since 1960, CO abundances have decreased at a rate of $5.7 \pm 0.3\%\,yr^{-1}$, roughly a factor of 2 more rapidly than NO_x, corresponding to a factor of 19 decrease in CO between 1960 and 2010 [e.g., *Warneke et al.*, 2012]. The overall rate of change from CO measurements in the SoCAB is consistent with a nationwide decrease in urban CO abundances of $5.2 \pm 0.8\%\,yr^{-1}$ observed between 1989 and 1999 by *Parrish et al.* [2002]. Observed CO trends in the SoCAB are consistent with those predicted in the CARB emissions inventory (e.g., annual average decrease in CO of $4.9 \pm 0.4\%\,yr^{-1}$ from all sources and $5.8 \pm 0.5\%\,yr^{-1}$ from on-road mobile sources) [*CARB*, 2009, accessed January 2013].

[29] For anthropogenic VOCs, an average rate of decrease of $7.3 \pm 0.7\%\,yr^{-1}$, corresponding to a decrease in average abundances by a factor of 44 over the 50 years, is determined using data from the Azusa and Upland SCAQMD stations and the ground-based field measurements since 1960 (Figure 4). This value, derived from two representative sites, is in quantitative agreement with a basin-wide average rate of decrease of $7.5\%\,yr^{-1}$ [*Warneke et al.*, 2012]. The annual average decrease in ROG of $6.2 \pm 0.4\%\,yr^{-1}$ between 1975 and 2010 solely from SoCAB on-road mobile sources in the CARB inventory (Table 5) is in better agreement with the ambient observations than is the annual average decrease of $4.4 \pm 0.4\%\,yr^{-1}$ determined from all sources in the CARB inventory.

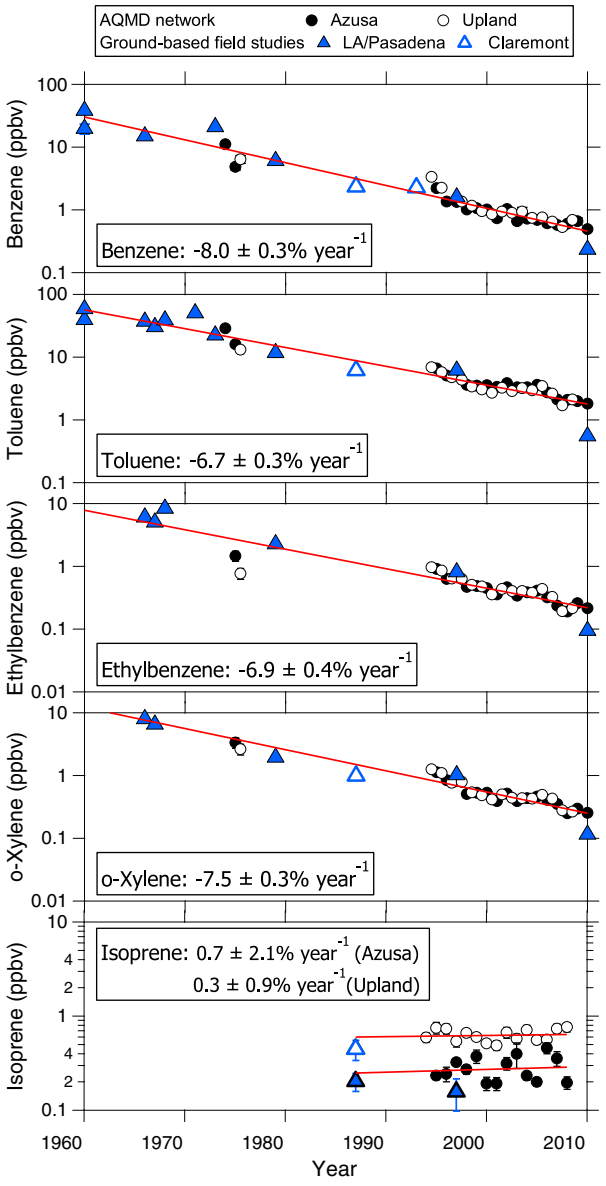

Figure 4. Average abundances of select NMOCs (in units of ppbv) measured at the Azusa (solid black circles) and Upland (open circles, offset by 0.5 years on *x* axis) surface network sites and ground-based field campaigns near LA/Pasadena (solid blue triangles) and Claremont (open blue triangles) since 1960. Error bars represent confidence limits based on the number of days of observations per year. LLS fits (red lines) represent long-term trends in abundances of speciated NMOCs. NMOCs related to vehicle exhaust have decreased at an average rate of 7.3% yr^{-1}. No significant change is observed for isoprene, an indicator of biogenic emissions.

[30] In contrast to anthropogenic VOCs, temporal trends in isoprene (Figure 4) show no statistically significant change since 1987 in the abundance of this biogenic VOC in the SoCAB. Additionally, no significant differences in average abundances of isoprene were observed from the arithmetic mean of the data from summertime weekday mornings (0500 and 0900 PDT) and weekday afternoons (1200 and 1800 PDT), when emissions of biogenic VOCs are most prominent [*Guenther et al.*, 1993].

3.2. Emissions Ratios

[31] Although many factors have contributed to changes in ambient concentrations of NO_x, CO, and VOCs over the years, decreasing abundances in the SoCAB are predominantly attributed to decreasing emissions from motor vehicles due to increasingly strict emissions standards in California [*Ban-Weiss et al.*, 2008; *Bishop and Stedman*, 2008; *Fujita et al.*, 2013; *Harley et al.*, 2005; *Lawson et al.*, 1990; *Lawson*, 2003; *McDonald et al.*, 2012; *Warneke et al.*, 2012]. Large decreases in motor vehicle emissions have occurred despite a factor of 2.4 increase in population (http://quickfacts.census.gov/qfd/states/06000.html) and a factor of 3 increase in fuel sales in the state of California since the 1960s [*Warneke et al.*, 2012]. In this section, we investigate the relative changes in precursor abundances and demonstrate their connection to changes in motor vehicle emissions by examining changes in observed emissions ratios.

3.2.1. Emissions Ratios to CO_2

[32] We start by comparing emissions ratios to CO_2 derived from near-tailpipe roadside measurements to airborne and ground-based measurements from field studies. Figure 5 illustrates changes over time in molar emission ratios of CO/CO_2, NO_x/CO_2, and (total HC)/CO_2 determined from the roadside observations since 1991 and from ambient observations from field studies since 1997 when ozone precursors and CO_2 were concurrently measured. As in previous studies [*Murphy et al.*, 2007; *Parrish et al.*, 2002; *Pollack et al.*, 2012], we use field observations of gas-phase NO_y when available as a more conserved tracer than NO_x for determining emissions ratios to long-lived atmospheric species such as CO and CO_2. Benzene is selected for comparison of ambient measurements of speciated VOC/CO_2 to roadside measurements of (total HC)/CO_2 due to its relatively slow reactivity with OH, thereby providing information about emissions independent of atmospheric processing or removal.

[33] The differences between roadside and ambient measurements reflect contributions from sources other than motor vehicles to total emissions of ozone precursors in the SoCAB. In Figure 5, ambient molar emission ratios of CO/CO_2 and NO_y/CO_2 are smaller than the corresponding emission ratios determined from near-tailpipe roadside measurements by an average percent difference of 37 ± 14% and 36 ± 9%, respectively. This difference indicates smaller relative contributions of on-road motor vehicles to total CO_2 emissions than to total CO and NO_x. According to 2008 California emission inventories [*CARB*, 2008a, accessed January 2013, 2008c, accessed January 2013], on-road motor vehicles are responsible for 53% of total CO and 49% of total NO_x in the SoCAB but only 35% of the total statewide CO_2 emissions. Assuming that the contribution from on-road motor vehicles to total CO_2 emissions in the SoCAB is the same as it is statewide (35%), we expect a 34% and 29% difference between roadside and ambient CO/CO_2 and NO_x/CO_2 measurements for the SoCAB. These differences are in close accord with the observations, which show a difference of 37 ± 14% for CO/CO_2 and 36 ± 9% for NO_x/CO_2, suggesting minimal variability between different measurement platforms and demonstrating the relative accuracy of the CARB emission inventories.

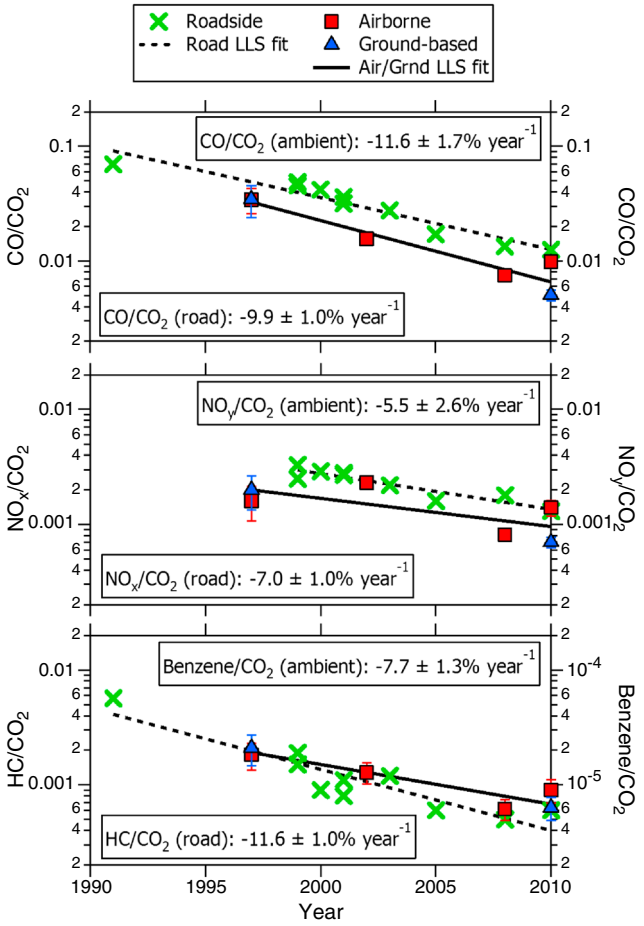

Figure 5. Molar emissions ratios of CO/CO_2, NO_x/CO_2, and HC/CO_2 (left axes) determined from roadside measurements (green crosses) and emissions ratios of CO/CO_2, NO_y/CO_2, and benzene/CO_2 (right axes) from airborne (red squares) and ground-based field measurements (blue triangles). LLS fits are indicated for roadside (dashed black line) and field (solid black line) measurements.

[34] Roadside measurements of CO/CO_2 and NO_x/CO_2 between 1991 and 2010 and ambient measurements of CO/CO_2 and NO_y/CO_2 between 1997 and 2010 decreased at similar rates, within the 1σ uncertainties of each determination (Figure 5 and Table 4). Larger differences are observed between trends in roadside measurements of (total HC)/CO_2 ($-11.6 \pm 1.0\%\,yr^{-1}$) and ambient measurements of benzene/CO_2 ($-7.7 \pm 1.3\%\,yr^{-1}$). Due to its toxicity, benzene has been selectively and progressively removed from fuels over the years, accounting for its disproportional change relative to CO. Regulatory efforts have resulted in a nationwide reduction of benzene relative to acetylene from vehicle exhaust by 40% between 1994 and 2002, corresponding to a reduction in benzene emissions by roughly 56% [*Fortin et al.*, 2005]. Fuel composition changes focused on minimizing benzene emissions between 1994 and 2002 contributed to the factor of 65 decrease in benzene abundances in the SoCAB observed between 1960 and 2010 (Figure 4). This specific focus on benzene approximately accounts for the greater decrease in ambient benzene abundances relative to the factor of 32 decrease in toluene abundances over the same 50 year period. Since benzene has decreased faster than most VOCs, we expect the rate of decrease in emissions ratios of benzene/CO_2 to represent an upper limit for decreases in ambient VOC/CO_2 ratios over time; however, (total HC) has decreased at a faster rate than benzene with respect to CO_2. Discrepancies between the trends may arise from the lack of ambient benzene/CO_2 data prior to implementation of regulatory efforts in 1994. Excluding the 1991 roadside data point from the LLS fit gives a rate of change for (total HC)/CO_2 of $-8.9 \pm 2.3\%\,yr^{-1}$, which is in better agreement with the decrease in ambient measurements of benzene/CO_2 ($-7.7 \pm 1.3\%\,yr^{-1}$). We also compare trends in molar emission ratios to CO_2 determined from roadside measurements, which targeted gasoline-fueled passenger vehicles, since 1991 to those predicted by the EMFAC2011-LDV emission inventory during summer between 1990 and 2010 (Table 5) [*CARB*, 2011, accessed January 2013]. Trends in roadside measurements (Table 4) agree reasonably with those from EMFAC2011-LDV (Table 5), demonstrating consistency between measurements and inventory emissions for light-duty vehicles. A slower decrease in NO_x/CO_2 ratio determined using EMFAC2011-SG (encompassing all on-road sources) compared to EMFAC2011-LDV shows that diesel-fueled vehicles are a significant contributor to on-road NO_x emissions [*Ban-Weiss et al.*, 2008; *McDonald et al.*, 2012]. From the difference in long-term trends from the EMFAC2011 inventory, we estimate that the presence of diesel-fueled vehicles has slowed the decrease of NO_x emissions from on-road mobile sources by $2.1 \pm 0.7\%\,yr^{-1}$ consistent with the ambient measurements that sampled all sources in the SoCAB.

3.2.2. Emissions Ratios to CO

[35] Next we look at trends in emissions ratios of select VOCs and NO_x relative to CO (Figure 6). A LLS fit of ambient enhancement ratios shows a statistically significant trend of $-1.2 \pm 0.4\%\,yr^{-1}$ since 1960 in benzene/CO but no significant trend ($-1.8 \pm 2.3\%\,yr^{-1}$) in (total HC)/CO ratio in roadside measurements since 1991 (Table 4). The differences are attributed to the temporal extent of the data record (e.g., ambient measurements since 1960 and roadside data only since 1991) as well as the faster decrease in emissions of benzene resulting from regulatory efforts initiated in the mid-1990s. The EMFAC2011-LDV emission inventory suggests no significant trend ($+0.1 \pm 0.1\%\,yr^{-1}$) for ROG/CO between 1990 and 2010, consistent with the lack of trend in the roadside measurements.

[36] Similarly, the long-term rate of change in ambient observations of benzene/CO can be compared with ROG/CO ratio determined for all sources in the SoCAB from the CARB emission inventory between 1975 and 2010 (Figure 6). Inventory-based ROG/CO ratios are presented on an arbitrary scale in Figure 6 and result in a small but significant rate of increase of $0.5 \pm 0.1\%\,yr^{-1}$. In contrast, ROG/CO ratio determined for on-road sources results in a small but significant rate of decrease ($-0.5 \pm 0.1\%\,yr^{-1}$). The long-term trends determined from the CARB inventory are inconsistent with the larger decrease in benzene/CO ($-1.2 \pm 0.4\%\,yr^{-1}$) from the ambient measurements, although the latter reflects the additional decrease in benzene due to regulatory efforts. In a similar analysis utilizing another long-lived and well-conserved tracer, *Warneke et al.* [2012] found little change in the ratio of acetylene/CO ($0.3 \pm 0.5\%\,yr^{-1}$) since 1960 (C. Warneke, personal communication, 2013).

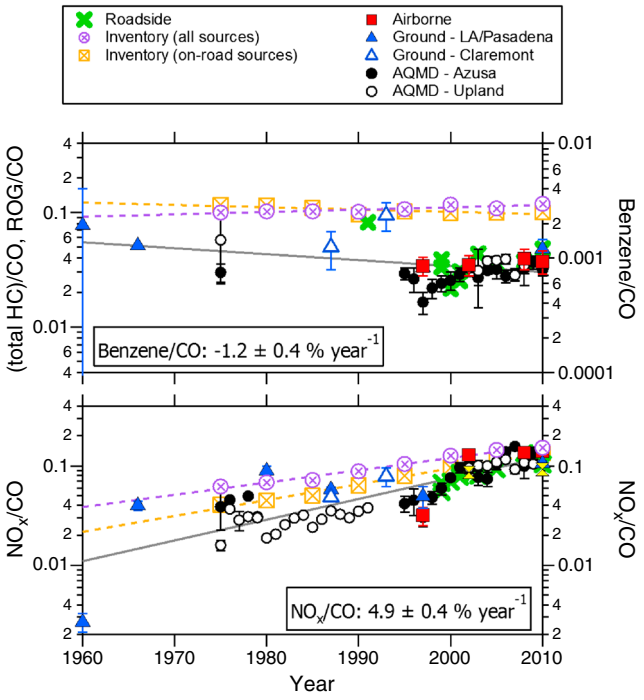

Figure 6. Ambient emissions ratios of VOC/CO and NO_x/CO (in units of ppbv/ppbv) determined from airborne measurements (red squares), ground-based field measurements near Azusa, Pasadena, and LA (solid blue triangles) and Claremont (open blue triangles), and surface network measurements for Azusa (solid black circles) and Upland (open black circles). Emission ratios of (total HC)/CO and NO_x/CO (green crosses) from roadside measurements and ROG/CO and NO_x/CO from the CARB emission inventory for all sources (purple symbols) and on-road sources (orange symbols) are also shown. Emission ratios of NO_x/CO from the various measurements are presented on a common scale. Ambient measurements of VOC/CO correspond with the right axis scale, roadside measurements of (total HC)/CO correspond with the left axis scale, and ROG/CO from the inventory is presented on an arbitrary scale. Solid lines represent the LLS fit to the combined ambient measurements; dashed lines represent LLS fits to the inventory data.

[37] Since regulatory efforts have led to additional reductions in benzene relative to other VOCs and CO from light-duty vehicles, we report trends in toluene, ethylbenzene, and *o*-xylene to further characterize changes in gasoline-fueled motor vehicle emissions over time. Although these VOCs are shorter-lived, we use data sampled during weekday mornings between 0500 and 0900 PDT to characterize VOC/CO ratios when emissions are at a maximum [*Parrish et al.*, 2002] and prior to extensive photochemical processing, as described in section 2.2. Ambient measurements show a slight increase in VOC/CO ratio over time (e.g., $+1.3 \pm 0.4\%\,yr^{-1}$ for toluene/CO, $+0.8 \pm 0.5\%\,yr^{-1}$ for ethylbenzene/CO, and $+0.5 \pm 0.5\%\,yr^{-1}$ for *o*-xylene/CO). Assuming these compounds have a common source and should show similar changes, an average of $+0.3 \pm 1.0\%\,yr^{-1}$ between 1960 and 2010 suggests there is no detectable trend in the average gasoline-fueled motor vehicle VOC/CO emissions ratio. This is in general agreement with a trend of $-1.7 \pm 1.0\%\,yr^{-1}$ determined from the rates of change in abundances of VOCs ($-7.3 \pm 0.7\%\,yr^{-1}$) and CO ($-5.7 \pm 0.3\%\,yr^{-1}$) using the combined observations (Table 4). *Warneke et al.* [2012] found the ratios to CO relatively constant for all VOCs in the LA basin since 1960. The long-term rate of increase of $0.5 \pm 0.1\%\,yr^{-1}$ for ROG/CO in the SoCAB determined from the CARB emission inventory between 1975 and 2010 is in agreement with the combined observations of VOC/CO ($+0.3 \pm 1.0\%\,yr^{-1}$) from the ambient measurements since 1960.

[38] Emissions ratios of NO_y/CO from roadside and ambient measurements are also shown in Figure 6. The observed increase in NO_x/CO emissions ratio follows from the faster decrease in CO emissions (average of $5.7\%\,yr^{-1}$) compared to the decrease in NO_x (average of $2.6\%\,yr^{-1}$) even though the atmospheric abundances of both have decreased significantly since 1960. LLS fit of the combined ambient and roadside measurements shows a positive trend in the NO_x/CO emissions ratio of $4.9 \pm 0.4\%\,yr^{-1}$ between 1960 and 2010

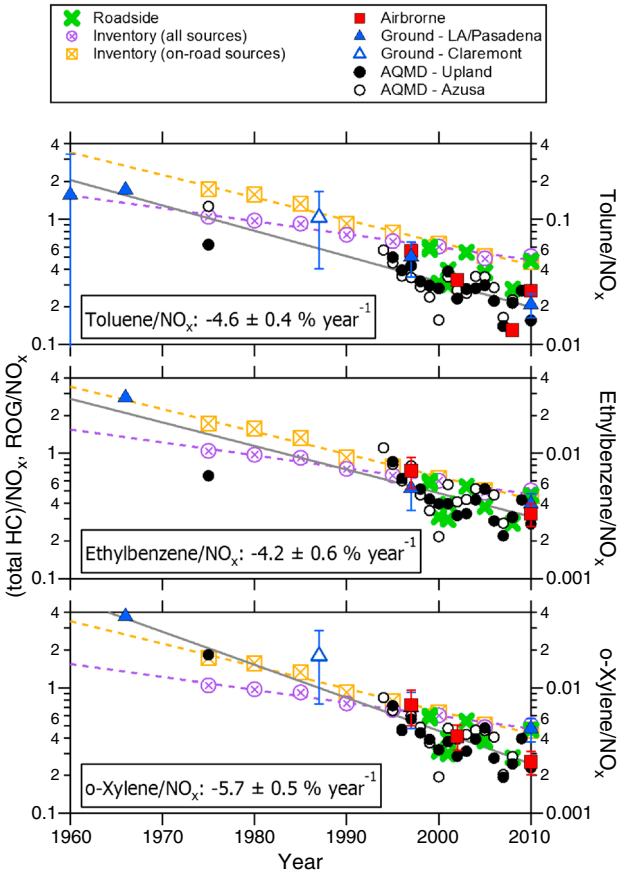

Figure 7. Ambient VOC/NO_x ratio (units of ppbv/ppbv, right axes scales) for airborne (red squares), ground-based field measurements near Azusa, Pasadena, and LA (solid blue triangles) and Claremont (open blue triangles), and surface network measurements for Azusa (solid black circles) and Upland (open black circles). Roadside measurements of (total HC)/NO_x (green crosses on left axis); emission ratios of ROG/NO_x from the CARB emission inventory for all sources (purple symbols) and on-road sources (orange symbols) are presented on an arbitrary scale. Solid lines represent the LLS fits to the combined ambient measurements; dashed lines represent LLS fits to the inventory data.

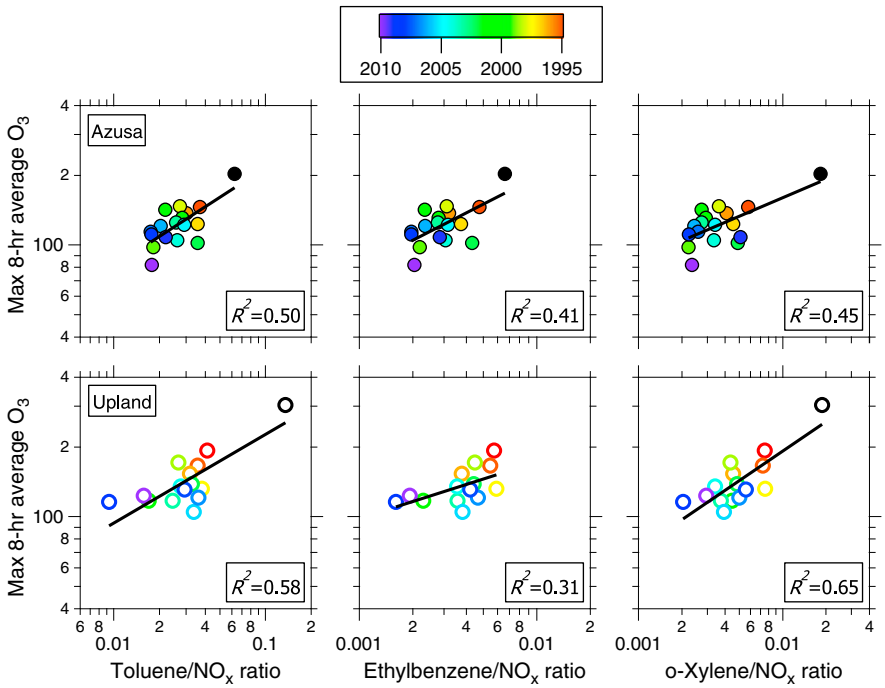

Figure 8. Maximum 8 h average ozone (in units of ppbv) versus VOC/NO_x ratios (in units of ppbv/ppbv) from the Azusa (solid symbols) and Upland (open symbols) network monitoring sites. Decreasing ozone is correlated with decreasing VOC/NO_x ratio from 1994 (red) to 2010 (purple); data from 1975 (black) are also shown where available. Solid black lines represent LLS fits of the data points; also reported are the R^2 values determined from each fit.

(Table 4). This value is larger than the trend of $3.3 \pm 0.5\%$ yr^{-1} based on the relative rates of decrease in NO_x and CO abundances. The rate of increase in NO_x/CO from the ambient field measurements ($5.2 \pm 1.4\%\,yr^{-1}$) is in agreement with that determined from the roadside measurements but larger than the long-term rate of change in NO_x/CO ratio predicted between 1975 and 2010 for the SoCAB by the CARB emission inventory ($3.7 \pm 0.2\%\,yr^{-1}$ for on-road sources and $2.9 \pm 0.2\%\,yr^{-1}$ for all sources) (Table 5).

[39] Absolute emission ratios of NO_x/CO predicted by the CARB emission inventory, which are included in Figure 6, are larger than that determined from the combined observations. Overestimates of NO_x/CO ratio from the inventory decrease from a factor of 4.3 for all sources and 2.8 for on-road sources in 1990 to a factor of 1.9 and 1.6, respectively, in 2010. These differences must reflect significant error(s) in the inventory. In contrast, top-down estimates of emissions ratios of NO_y/CO for weekdays in 2002 and 2010 in the LA basin using an inverse model [*Brioude et al.*, 2012] show better agreement with absolute emission ratios determined from the field measurements (e.g., NO_y/CO ratios simulated for 2002 and 2010 are underestimated by an average factor of 1.5). The long-term rate of change in measured weekday ambient NO_x/CO is also in agreement with that determined from the EMFAC2011-SG inventory ($4.6 \pm 0.9\%\,yr^{-1}$), which combines emissions from gasoline-fueled and diesel-fueled vehicles [*Pollack et al.*, 2012]. However, there is less agreement between the long-term increase in roadside measurements of NO_x/CO from light-duty vehicles ($5.9 \pm 1.3\%$ yr^{-1}) and the rate of increase determined from the EMFAC2011-LDV inventory ($2.5 \pm 0.3\%\,yr^{-1}$).

[40] Here we have utilized long-lived, well-conserved species to make direct correlations between abundances and emissions ratios measured in the SoCAB. Consistency between trends derived from near-tailpipe roadside and from ambient measurements confirms on-road motor vehicles as the predominant source of CO, VOC, and NO_x emissions in the SoCAB. Agreement between trends in measured emissions ratios and atmospheric abundances demonstrates that changes in ambient concentrations in the SoCAB continue to reflect changes in emission rates of precursor species. This analysis has shown that all of the long-term trends in emissions, except for NO_x, are underestimated by the CARB inventory for all sources in the SoCAB. In contrast, all of the long-term rates of change predicted by EMFAC2011-LDV, with the exception of NO_x/CO ratio, agree reasonably with the long-term trends determined from the roadside measurements of light-duty vehicles emissions. Differences between long-term trends from the measurements and emission inventories suggest that statistically significant errors still exist in the inventories.

3.2.3. VOC/NO_x Ratio

[41] Larger reductions in emissions of VOCs relative to NO_x over time have resulted in decreasing VOC/NO_x emission ratios in the SoCAB over the past five decades. Data from the monitoring network and from intensive field measurements (Figure 7) show the trends in toluene, ethylbenzene, and *o*-xylene emissions relative to NO_x. These three VOCs are selected as compounds characteristic of vehicle exhaust with OH reaction rate coefficients similar to that for NO_2 [*Sander et al.*, 2006], such that

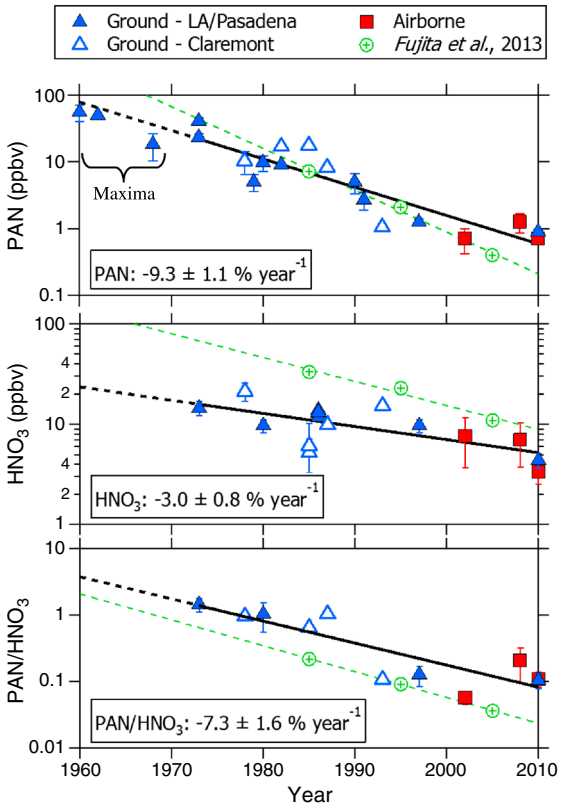

Figure 9. Changes in average abundances of PAN and HNO_3 and enhancement ratios of PAN/HNO_3 since 1973 using data from airborne (red squares) and ground-based field studies near Los Angeles (solid blue triangles) and Claremont (open blue triangles). Observed PAN maxima between 1960 and 1970 are included in the upper plot but excluded from the LLS fit (solid black lines); however, the extrapolated LLS fit to 1960 (dashed black lines) is in agreement with those observations. Values predicted by box model simulations [*Fujita et al.*, 2013] (green symbols and dashed lines) are shown in comparison to the measurements.

VOC/NO_x emissions ratios should be approximately preserved during processing by OH. Additionally, as noted above, we minimize chemical processing of the emissions prior to analysis by selectively using data from weekday mornings. A trend of $-4.8 \pm 0.9\%\,yr^{-1}$ for these VOC/NO_x ratios is derived from network and field measurements, consistent with the value of $-4.5 \pm 0.8\%\,yr^{-1}$ calculated from observed trends in VOC and NO_x abundances. This trend is significantly larger than $-2.3 \pm 0.2\%\,yr^{-1}$ in the unspeciated ROG/NO_x emissions ratio predicted by the CARB inventory for all sources in the SoCAB between 1975 and 2010. The discrepancy between observed and inventory values is consistent with *Fujita et al.* [2013], who reported that ambient measured NMOC/NO_x ratios from SCAQS 1987, SCOS 1997, and field measurements in 2009 are about a factor of 2 higher than the emission inventory ratios. Although a trend of $-2.4 \pm 0.4\%\,yr^{-1}$ in ROG/NO_x ratio is predicted by the EMFAC2011-LDV emission inventory [*CARB*, 2011, accessed January 2013] between 1990 and 2010, roadside data since 1991 show no significant trend ($2.0 \pm 2.7\%$ yr^{-1}) in (total HC)/NO_x emissions ratio (Table 4). Trends in ambient VOC/NO_x ratios (average of -4.8 $0.9\%\,yr^{-1}$) are in agreement with changes of -4.2 $0.9\%\,yr^{-1}$ in ROG/NO_x ratio determined from the EMFAC2011-SG emission inventory, which reflects combined emissions from light-duty gasoline-fueled and heavy-duty diesel-fueled vehicles.

4. Causes of Decreasing Ozone in the SoCAB

[42] Ozone formation in the SoCAB strongly depends on abundances of anthropogenic VOCs and NO_x and on the VOC/NO_x ratio [*Fujita et al.*, 2003; *Fujita et al.*, 2013; *Lawson*, 2003; *Pollack et al.*, 2012]. Figure 8 shows positive correlations between decreasing maximum 8 h ozone concentrations and decreasing VOC/NO_x ratio since 1975 from the Azusa and Upland surface network data sets. However, the causal relationships between decreasing ozone and decreasing precursor emissions, and their ratios, remain unclear. In the following sections, we use historical measurements of secondary oxidation products to better identify the major causes of decreasing ozone in the SoCAB. We analyze ambient measurements of secondary pollutants from summertime weekday afternoons between 1200 and 1800 PDT when photochemical processing is well advanced and the planetary boundary layer is well developed. We assume negligible influence from any changes in meteorological conditions that might affect average atmospheric residence times in the SoCAB, dilution, pollutant carryover, transport, and deposition over those 50 years. As discussed in sections 4.2 and 4.3, this approach is supported by airborne measurements from CalNex 2010, ARCTAS 2008, and ITCT 2002, which show no statistically significant difference in NO_y/CO and NO_y/CO_2 emissions ratios throughout the sampling duration of each flight (typically 1000 to 1800 PDT) and between the eastern and western geographic portions of the SoCAB over the past decade.

4.1. Long-Term Trends in NO_x Oxidation Products

[43] Atmospheric PAN is a result of HO_x radical chemistry and is positively correlated with ozone production [*Pollack et al.*, 2012; *Roberts et al.*, 2007; *Roberts et al.*, 1995; *Sillman*, 1995]. Thermal decomposition of PAN regenerates RO_2 and NO_2 and promotes continued ozone production. In contrast, formation of HNO_3 removes OH radicals from the chain reactions that produce ozone, and thus atmospheric HNO_3 is a result of chemical reactions that terminate the ozone formation cycle. The abundance of PAN relative to HNO_3 provides an indication of the balance between propagation and termination of the catalytic ozone formation cycle.

[44] The temporal trends of the average abundances of PAN and HNO_3 since 1973 from the available airborne and ground-based measurements are illustrated in Figure 9. PAN maxima prior to 1973 reported in the literature are also shown in the figure, although they are not included in the determination of the long-term trend. Although concentrations of secondary pollutants may vary significantly with location in the SoCAB, the data in Figure 9 show no systematic difference in abundances of PAN measured at these selected locations in the SoCAB. Measured abundances of PAN exhibit an average trend of $-9.3 \pm 1.1\%\,yr^{-1}$ since 1973 (Table 6), corresponding to a factor of 34 decrease between 1973 and

Table 6. Rate of Change (Δ) and Corresponding 1σ Standard Deviation in Units of Percent Change Per Year for Abundances and Enhancement Ratios of Secondary Oxidation Products Determined From the Airborne and Ground-Based Field Measurements Since 1973 and Values Predicted by *Fujita et al.* [2013] for 1985, 1995, and 2005 Using a Chemical Box Model[a]

	Field Observations			Model Predicted		
Measurement	Δ (% yr^{-1})	r^2	N	Δ (% yr^{-1})	r^2	N
PAN	-9.3 ± 1.1	0.82	15	-13.5 ± 1.1	0.99	3
HNO_3	-3.0 ± 0.8	0.47	16	-5.3 ± 1.0	0.96	3
PAN/HNO_3	-7.3 ± 1.6	0.74	11	-8.6 ± 0.1	1.00	3
$O_3/(PAN+HNO_3)$	0.8 ± 1.4	0.04	10	-1.1 ± 0.6[b]	0.75	3
$O_x/(PAN+HNO_3)$	-1.4 ± 1.3	0.14	9			
NO_x/NO_y	-0.9 ± 0.9	0.77	10			
$(PAN+HNO_3)/NO_y$	2.2 ± 0.5	0.68	10	-3.0 ± 2.2	1.00	3
PAN/NO_y	-2.0 ± 1.4	0.20	10	-10.6 ± 0.5	1.00	3
HNO_3/NO_y	3.3 ± 1.0	0.56	10	-2.3 ± 0.4	0.97	3

[a]A negative rate of change signifies a decreasing trend over time; N represents the number of data points, corresponding to years of data, used for linear regression.
[b]LLS fit of values predicted for $O_3/(NO_y\text{-}NO_x)$ [*Fujita et al.*, 2013].

2010. PAN was first identified as a particularly important eye irritant in Los Angeles smog [*Leighton*, 1961]. PAN abundances have decreased much more rapidly than ozone (e.g., factor of 34 reduction in PAN versus factor of 2.9 reduction in O_3 over the same 37 year period), demonstrating much greater progress in reducing some compounds of concern for air quality compared to O_3.

[45] Previous studies [*Kelly*, 1992; *Russell et al.*, 1988b; *Spicer*, 1983] have shown direct correlation between reductions in PAN, which is produced from VOC oxidation in the presence of NO_x, and reductions in both VOC and NO_x precursors. The observed trend in PAN since 1973 of $-9.3 \pm 1.1\%\,yr^{-1}$ is quantitatively similar to the rate of change in the product of the trends in its precursors ($-9.7 \pm 0.7\%\,yr^{-1}$), calculated from the sum of the slopes of the long-term trends of VOC and NO_x since 1960 (Table 4) and using equation (4). The difference may be attributed to our selection of VOCs for the combined trend reported in Table 4, which does not include acetaldehyde, the direct precursor to PAN formation. Analysis of the trend in acetaldehyde results in a decrease of $7.3 \pm 1.6\%\,yr^{-1}$ in the SoCAB, although this is based solely on measurements after 1980. A similar decrease is observed for formaldehyde, which serves as an indicator for formation of secondary organic products. Analysis of formaldehyde maxima [*Grosjean*, 1982] dating back to 1960 shows an average trend of $-7.6 \pm 1.0\%\,yr^{-1}$, consistent with that calculated by averaging trends in directly emitted benzene, toluene, ethylbenzene, and *o*-xylene ($-7.3 \pm 0.7\%\,yr^{-1}$) (Table 4). The observed PAN trend since 1973 ($-9.3 \pm 1.1\%\,yr^{-1}$) is in agreement with the product of the decrease in abundances of formaldehyde and NO_x ($10.0 \pm 1.0\%\,yr^{-1}$).

[46] Average abundances of HNO_3 have changed at a rate of $-3.0 \pm 0.8\%\,yr^{-1}$ (Table 6), corresponding to a factor of 3.1 decrease between 1973 and 2010. Reductions in HNO_3 concentrations have been found to be directly proportional to decreases in NO_x [*Kelly*, 1992; *Russell et al.*, 1988b; *Spicer*, 1983]. The trend in HNO_3 agrees within statistical uncertainty with the average rate of decrease determined for NO_x ($-2.6 \pm 0.3\%\,yr^{-1}$). As found for PAN, average HNO_3 abundances in Figure 9 show no dependence on the locations selected to represent the SoCAB in this analysis. The faster rate of decrease in PAN relative to HNO_3 since 1973 results in a trend in enhancement ratios of PAN/HNO_3 of $-7.3 \pm 1.6\%\,yr^{-1}$. Owing to the positive correlations of PAN with ozone production and HNO_3 with radical termination, long-term decreases in the relative concentrations of PAN and HNO_3 indicate that decreasing ozone concentrations in the SoCAB are a direct result of decreasing photochemical production of ozone due to decreasing abundances of VOC and NO_x precursors.

[47] Also shown in Figure 9 are abundances of PAN and HNO_3 simulated for 1985, 1995, and 2005 in the SoCAB using a chemical box model [*Fujita et al.*, 2013]. While simulated abundances of PAN are consistent with the measured values, simulated abundances of HNO_3 are overestimated by roughly a factor of 3. The model also predicts significantly larger rates of decrease in PAN and HNO_3 than the apparent trends in the ambient measurements (Table 6).

4.2. Change in Ozone Production Efficiency

[48] In this section, we investigate the contribution of changes in ozone production efficiency (OPE) to the observed decreases in ozone abundances over time. We take the slope of a LLS fit of O_3 versus the sum of the major NO_x oxidation products ($PAN + HNO_3$) to provide a measure of ozone produced per NO_x oxidized [*Trainer et al.*, 1993]. Figure 10 shows a scatter plot of O_3 versus ($PAN + HNO_3$) using the available field measurements in the SoCAB since 1973. LLS fits result in large variability in the slopes determined from each data set. Given the variability in fitted slopes between data sets, this analysis finds no significant trend in derived OPE between 1973 and 2010. LLS slopes from scatter plots of odd oxygen ($O_x = O_3 + NO_2$) versus

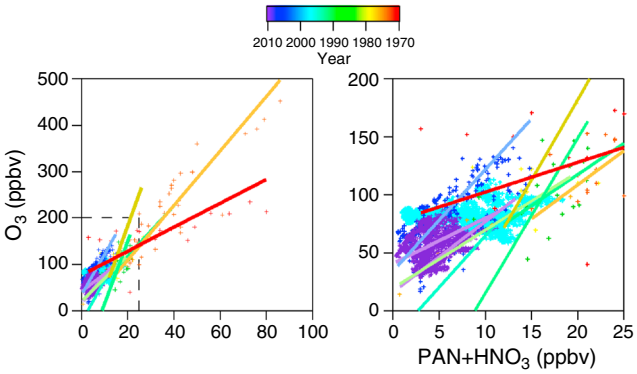

Figure 10. Correlation plots of O_3 versus ($PAN + HNO_3$) using airborne and ground-based measurements from field studies between 1973 (red) and 2010 (purple), with the right plot showing an expanded view of the region inside the dashed boxed from the left plot. Ground-based measurements include data reported by *Spicer* [1977b], *Tuazon et al.* [1981], *Hanst et al.* [1982], and *Grosjean* [1986] and from the SCAQS (1987), LAAFRS (1993), SCOS (1997), and CalNex (2010) field campaigns; airborne measurements include data from ITCT (2002), ARCTAS-CARB (2008), and CalNex (2010). Solid lines represent LLS ODR of each data set corresponding by color; a time series of the slopes is presented in Figure 11.

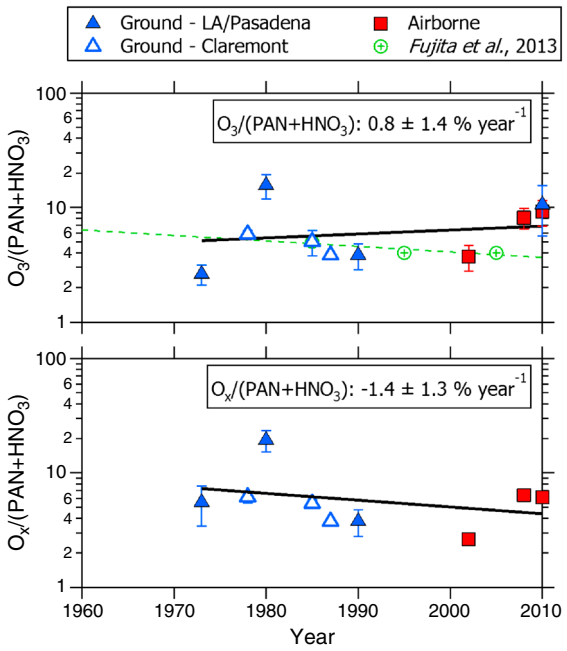

Figure 11. Changes in $O_3/(PAN+HNO_3)$ and $O_x/(PAN+HNO_3)$ since 1973 using data from airborne (red squares) and ground-based (blue triangles) field studies near Los Angeles (solid blue triangles) and Claremont (open blue triangles). Values predicted by box model simulations [*Fujita et al.*, 2013] (green symbols and dashed lines) are shown in comparison to the measurements. Assuming no loss of NO_y species, LLS fits show no significant change since 1973 (solid black lines).

$(PAN+HNO_3)$ are also shown in Figure 11. O_x has been interpreted in previous studies as a more conserved measure of net oxidant production [*Johnson*, 1984; *Murphy et al.*, 2007; *Pollack et al.*, 2012; *Tonse et al.*, 2008] and is used here to isolate the relative contributions from titration and net photochemical production to observed ozone levels. No detectable trend in $O_3/(PAN+HNO_3)$ and $O_x/(PAN+HNO_3)$ suggests that over the 37 years spanned by the data, OPE has remained constant within our ability to quantify from the available data. Model-predicted ratios for $O_3/(NO_y\text{-}NO_x)$ reported by *Fujita et al.* [2013], also shown in Figure 11, agree well with the measured ratios and further indicate no detectable change in OPE over time.

[49] The above calculations assume no differential loss of NO_y species. However, OPE interpreted from these slopes will be overestimated if a significant fraction of any gas-phase NO_y species, e.g., HNO_3, is removed from the atmosphere prior to measurement [*Ryerson et al.*, 1998; *Trainer et al.*, 1993]. Although minimal loss of NO_y species in the SoCAB is justified by the minimal change observed in ratios of NO_y/CO and NO_y/CO_2 over the spatial extent of the basin and the temporal extent of sampling using the airborne data sets, we also consider the influence of loss of HNO_3 on the derived OPE. Since HNO_3 is highly soluble, it is subject to removal by wet and dry deposition, and it can also form ammonium nitrate aerosol. We have recalculated OPE assuming 50% loss of HNO_3 prior to measurement, which results in larger positive biases in OPE for years between 1990 and 2010 where HNO_3 is a larger fraction of NO_y. Even under this extreme example, HNO_3 loss does not significantly affect the long-term LLS fit. With or without HNO_3 loss, we detect no significant change in OPE between 1973 and 2010 based on analysis of the ambient data.

[50] The lack of a discernible trend in derived OPE since 1973 (Figure 11 and Table 6) contradicts an expected decrease due to the decreasing VOC/NO_x ratio. Studies of weekday-weekend differences in ozone in the SoCAB have shown decreasing OPE with decreasing VOC/NO_x ratio on weekdays versus weekends [*Fujita et al.*, 2013; *Pollack et al.*, 2012]. However, the observed changes in VOC/NO_x ratio in these studies are primarily driven by weekend reductions in NO_x with little weekday-weekend difference in VOCs. Past studies [*Lin et al.*, 1988; *Liu et al.*, 1987; *Roberts et al.*, 2007; *Roberts et al.*, 1995; *Ryerson et al.*, 1998; *Ryerson et al.*, 2001; *Trainer et al.*, 1993] have shown that the amount of ozone produced per NO_x oxidized depends nonlinearly on NO_x and VOC concentrations, such that OPE at a fixed VOC/NO_x ratio increases with decreasing abundances of NO_x. Here we suggest that the net effect of decreasing NO_x abundances and simultaneously decreasing VOC/NO_x ratio over time in the SoCAB have effectively canceled, resulting in minimal change in OPE over the past 50 years.

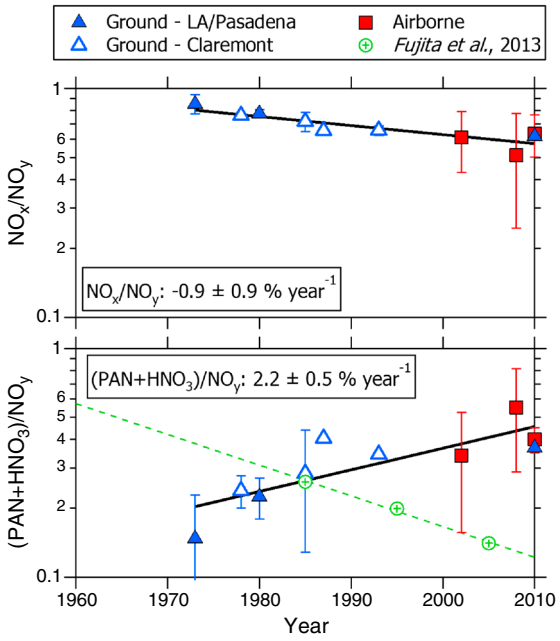

Figure 12. Changes in the fraction of unreacted NO_x and NO_x oxidation products $(PAN+HNO_3)$ relative to total reactive nitrogen (NO_y) using data from airborne (red squares) and ground-based (blue triangles) field studies near Los Angeles (solid blue triangles) and Claremont (open blue triangles). Values predicted by box model simulations [*Fujita et al.*, 2013] (green symbols and dashed lines) are shown in comparison to the measurements. Assuming no loss of NO_y species, LLS fits (solid black lines) of the long-term trends show an average decrease in unreacted NO_x ($-0.9\%\,yr^{-1}$) and an average increase in NO_x oxidation products ($2.2\%\,yr^{-1}$) since 1973.

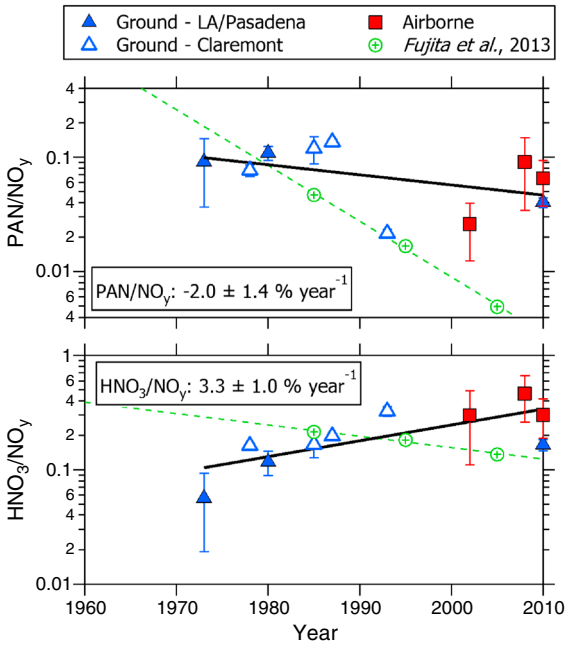

Figure 13. Changes in the fraction of PAN and HNO_3 relative to total reactive nitrogen (NO_y) using data from airborne (red squares) and ground-based (blue triangles) field studies near Los Angeles (solid blue triangles) and Claremont (open blue triangles). Values predicted by box model simulations [*Fujita et al.*, 2013] (green symbols and dashed lines) are shown in comparison to the measurements. Assuming no loss of NO_y species, LLS fits (solid black lines) of the long-term trends show an average decrease in PAN ($-2.0\%\,yr^{-1}$) and an average increase in HNO_3 ($3.3\%\,yr^{-1}$) since 1973.

4.3. Changes in Rate of Photochemical Processing

[51] Assuming atmospheric mixing and residence times in the SoCAB have not changed in the last 50 years, changes in the fraction of oxidized NO_x relative to NO_y indicate differences in the rate of photochemical processing of NO_x over time [*Pollack et al.*, 2012]. Figure 12 presents the data since 1973 in two coupled ways: the measured NO_x to NO_y ratio in the top panel illustrates changes in the average fraction of unreacted NO_x, while measured $(PAN + HNO_3)$ to NO_y ratio in the bottom panel illustrates changes in the average fraction of NO_x oxidation products to NO_y. As discussed in section 2.1.3, measured gas-phase NO_y data are used where available; the sum of individually measured gas-phase NO_y constituent species ($\sum NO_y$; typically $NO_x + PAN + HNO_3$) is used otherwise. Alkyl nitrates were not measured in most of the field studies used in this analysis and thus are not incorporated into $\sum NO_y$ but are assumed to be a relatively small contribution to total NO_y in the Los Angeles basin. LLS fit to these data suggests a statistically insignificant trend of $-0.9 \pm 0.9\%\,yr^{-1}$ in the fraction of unreacted NO_x in the SoCAB between 1973 and 2010 (Table 6). On the other hand, we observe a significant increase in the fraction of oxidized NO_x of $2.2 \pm 0.5\%\,yr^{-1}$. This result is robust to recalculation of the $(PAN + HNO_3)/NO_y$ trend assuming 50% loss of HNO_3 prior to gas-phase measurement and suggests that this trend is insensitive to the fraction of HNO_3 in NO_y. In contrast, ratios of $(PAN + HNO_3)/NO_y$ derived from box model simulations in *Fujita et al.* [2013] show a decreasing trend in the fraction of oxidized NO_x (Figure 12 and Table 6) and are inconsistent with the increasing trend derived from the ambient data.

[52] The ambient data suggest that atmospheric photochemical processing of NO_x in the SoCAB has increased over the 37 years spanned by the available measurements. The increase in the fraction of oxidized NO_x since 1973 indicates more rapid processing of NO_x as a result of the large changes in amount and proportion of emissions in the Los Angeles basin. Along with faster photochemical processing, emissions changes have resulted in increasingly favored production of HNO_3 over time, demonstrated by a derived positive trend of $3.3 \pm 1.0\%\,yr^{-1}$ in HNO_3/NO_y and a trend of $-2.0 \pm 1.4\%\,yr^{-1}$ in PAN/NO_y (Figure 13 and Table 6).

[53] Differences between measured and simulated ratios [*Fujita et al.*, 2013] of HNO_3/NO_y and PAN/NO_y are also illustrated in Figure 13. The differences in PAN/NO_y ratio likely reflect the model's overestimate of HNO_3.

5. Summary

[54] We quantify long-term trends in abundances and emissions ratios of precursors and secondary oxidation products in the SoCAB using data from a surface monitoring network, roadside monitors, ground-based field sites, and research aircraft. Consistency in average abundances and emission ratios determined from the various platforms over the past 50 years permits quantification of long-term trends in emissions in the South Coast Air Basin. Agreement between near-tailpipe measurements by roadside monitors, basin-wide measurements from aircraft, and local assessments from ground-based measurements and surface network sites confirms motor vehicles as the predominant source of precursor emissions in the SoCAB. Differences between long-term trends determined from the ambient measurements and emission inventories suggest that significant errors still exist in the inventories. A decrease in VOC/NO_x ratio is observed since the 1960s and is a direct result of the faster decrease in VOC emissions compared to NO_x. Decreasing maximum 8 h ozone concentration in the SoCAB is positively correlated with decreasing ozone precursor abundances and VOC/NO_x ratio over the past 50 years. The well-established connection between O_3 and PAN production allows use of the trends in NO_x oxidation products as a tool for relating long-term changes in ozone production to changes in precursor emissions. The observed decreases in NO_x oxidation products, PAN and HNO_3, over time are consistent with decreasing VOC and NO_x abundances. No change in enhancement ratios of O_3 and $(O_3 + NO_2)$ to $(PAN + HNO_3)$ over time suggests no detectable trend in ozone production efficiency since 1973, although there is wide variability in the results from different data sets. The trend in NO_x oxidation products demonstrates an increase in the fraction of oxidized NO_x since 1973, suggesting that atmospheric oxidation rates of NO_x have increased over time as a result of the emissions changes in the SoCAB. Trends in the fractions of PAN and HNO_3 relative to NO_y show that HNO_3 production has been increasingly favored over time.

[55] This analysis demonstrates that significant reductions in secondary pollutants have been the direct result of reduced precursor emissions, with the largest changes related to increased emission standards and improved technology in

motor vehicles. Through the decades, VOCs were the initial primary target for emissions reductions in the SoCAB, followed more recently by increasing efforts to control NO_x. As shown in our assessment and previous analyses, these control measures have been effective in reducing ambient ozone levels over the past 50 years. Stricter emissions standards for diesel-fueled vehicles are designed to further reduce NO_x emissions [*CARB*, 2008b; *McDonald et al.*, 2012]. Overall, the observations from this analysis suggest that reductions in ozone and other secondary pollutants in the SoCAB over the past 50 years are a direct result of decreasing abundances of VOCs and NO_x and VOC/NO_x ratio and that ozone continues to be responsive to local emissions control strategies in the Los Angeles basin.

[56] **Acknowledgments.** The authors thank L. Dolislager, B. Weller, and D. Oda from the California Air Resources Board for providing historical data from the SCAQMD and PAMS surface monitoring networks and various field studies in the SoCAB. We also thank G. Bishop and D. Stedman for help with conversion and interpretation of the roadside measurements.

References

Altshuller, A. P., et al. (1971), Hydrocarbon composition of atmosphere of Los Angeles basin—1967, *Environ. Sci. Technol.*, *5*(10), 1009–1016.

Anlauf, K. G., et al. (1991), Intercomparison of atmospheric nitric-acid measurements at elevated ambient concentrations, *Atmos. Environ., Part A*, *25*(2), 393–399, doi:10.1016/0960-1686(91)90310-4.

Ban-Weiss, G. A., et al. (2008), Long-term changes in emissions of nitrogen oxides and particulate matter from on-road gasoline and diesel vehicles, *Atmos. Environ.*, *42*(2), 220–232, doi:10.1016/j.atmosenv.2007.09.049.

Beaton, S. P., et al. (1995), On-road vehicle emissions—Regulations, costs, and benefits, *Science*, *268*(5213), 991–993, doi:10.1126/science.268.5213.991.

Bishop, G. A., and D. H. Stedman (2008), A decade of on-road emissions measurements, *Environ. Sci. Technol.*, *42*(5), 1651–1656, doi:10.1021/Es702413b.

Bishop, G. A., et al. (2010), On-road emission measurements of reactive nitrogen compounds from three California cities, *Environ. Sci. Technol.*, *44*(9), 3616–3620, doi:10.1021/Es903722p.

Bishop, G. A., et al. (2012), Multispecies remote sensing measurements of vehicle emissions on Sherman Way in Van Nuys, California, *J. Air Waste Manage. Assoc.*, *62*(10), 1127–1133.

Blumenthal, D. (1999), *Measurements Made Aloft by a Twin-Engine Aircraft to Support the SCOS97-NARSTO Study*, Report submitted by Sonoma Technol., Calif. Air Resour. Board, *96-309*.

Boggs, P. T., et al. (1987), A stable and efficient algorithm for nonlinear orthogonal distance regression, *SIAM J. Sci. Stat. Comput.*, *8*, 1052–1078.

Brioude, J., et al. (2012), Top-down estimate of surface flux in the Los Angeles Basin using a mesoscale inverse modeling technique: Assessing anthropogenic emissions of CO, NO_x and CO_2 and their impacts, *Atmos. Chem. Phys. Discuss.*, *12*, 31439–31481, doi:10.5194/acpd-12-31439-2012.

Bufalini, J. J., et al. (1972), Hydrogen-peroxide formation from formaldehyde photooxidation and its presence in urban atmospheres, *Environ. Sci. Technol.*, *6*(9), 816–821.

Burgard, D. A., et al. (2006), Spectroscopy applied to on-road mobile source emissions, *Appl. Spectrosc.*, *60*(5), 135a–148a.

California Air Resources Board (CARB) (2008a), California greenhouse gas emission inventory, Sacramento. [Available at http://www.arb.ca.gov/cc/inventory/inventory.htm].

California Air Resources Board (CARB) (2008b), California Code of Regulations: Regulation to reduce emissions of diesel particulate matter, oxides of nitrogen and other criteria pollutants, from in-use heavy-duty diesel-fueled vehicles, Title 13, Section 2025, Sacramento.

California Air Resources Board (CARB) (2008c), Statewide emission data, Sacramento. [Available at http://www.arb.ca.gov/ei/emissiondata.htm].

California Air Resources Board (CARB) (2009), California almanac of emissions and air quality—2009 edition, Sacramento. [Available at http://www.arb.ca.gov/aqd/almanac/almanac.htm].

California Air Resources Board (CARB) (2011), EMFAC2011 mobile source emission inventory, Sacramento. [Available at http://www.arb.ca.gov/msei/modeling.htm].

Croes, B. E., and E. M. Fujita (2003), Overview of the 1997 Southern California Ozone Study (SCOS97-NARSTO), *Atmos. Environ.*, *37*, S3–S26.

Dallmann, T. R., and R. A. Harley (2010), Evaluation of mobile source emission trends in the United States, *J. Geophys. Res.*, *115*, D14305, doi:10.1029/2010jd013862.

Darley, E. F., et al. (1963), Analysis of peroxyacyl nitrates by gas chromatography with electron capture detection, *Anal. Chem.*, *35*(4), 589–591.

Fehsenfeld, F. C., et al. (1990), Intercomparison of NO_2 measurement techniques, *J. Geophys. Res.*, *95*(D4), 3579–3597.

Finlayson-Pitts, B. J., and J. N. Pitts (2000), *Chemistry of the Upper and Lower Atmosphere: Theory, Experiments, and Applications*, Academic, San Diego, Calif.

Fujita, E. M., et al. (1992), Comparison of emission inventory and ambient concentration ratios of CO, NMOG, and NO_x in California South Coast Air Basin, *J. Air Waste Manage.*, *42*(3), 264–276.

Fitz, D. (1999), Surface and upper air VOC sampling and analysis during the 1997 Southern California oxidant study, report, Calif. Air Resour. Board, Sacramento.

Fitz, D. R. (2002), Evaluation of NO_y and nitric acid measurement methods and collection of ambient data, *Calif. Air Resour. Board*, Sacramento.

Fortin, T. J., et al. (2005), Temporal changes in U.S. benzene emissions inferred from atmospheric measurements, *Environ. Sci. Technol.*, *39*(6), 1403–1408.

Fujita, E. M., et al. (1999), *SCOS97-NARSTO 1997 Southern California Ozone Study and Aerosol Study*, Quality Assurance Plan, vol. II., Calif. Air Resour. Board, Sacramento.

Fujita, E. M., et al. (2003), Evolution of the magnitude and spatial extent of the weekend ozone effect in California's South Coast Air Basin, 1981–2000, *J. Air Waste Manage.*, *53*(7), 802–815.

Fujita, E. M., et al. (2013), Past and future ozone trends in California's South Coast Air Basin: Reconciliation of ambient measurements with past and projected emissions inventories, *J. Air Waste Manage.*, *63*(1), 54–69, doi:10.1080/10962247.2012.735211.

Gertler, A. W., et al. (1999), The impact of California Phase 2 Reformulated Gasoline on real-world vehicle emissions, *J. Air Waste Manage.*, *49*(11), 1339–1346.

Grosjean, D. (1982), Formaldehyde and other carbonyls in Los Angeles ambient air, *Environ. Sci. Technol.*, *16*(5), 254–262, doi:10.1021/Es00099a005.

Grosjean, D. (1983), Distribution of atmospheric nitrogenous pollutants at a Los Angeles area smog receptor-site, *Environ. Sci. Technol.*, *17*(1), 13–19.

Grosjean, D. (1986), Measurements of inorganic nitrate, aldehydes and carboxylic-acids during the NSMCS study, *Abstr. Pap. Am. Chem. Soc.*, *192*, 128-ENVR.

Grosjean, D. (1988), Aldehydes, carboxylic-acids and inorganic nitrate during NSMCS, *Atmos. Environ.*, *22*(8), 1637–1648.

Grosjean, D. (2003), Ambient PAN and PPN in Southern California from 1960 to the SCOS97-NARSTO, *Atmos. Environ.*, *37*, S221–S238, doi:10.1016/S1352-2310(03)00392-3.

Grosjean, D., et al. (1993), Peroxyacyl nitrates at Southern California mountain forest locations, *Environ. Sci. Technol.*, *27*(1), 110–121.

Grosjean, E., et al. (2001), Peroxyacetyl nitrate and peroxypropionyl nitrate during SCOS97-NARSTO, *Environ. Sci. Technol.*, *35*(20), 4007–4014.

Guenther, A. B., et al. (1993), Isoprene and monoterpene emission rate variability: Model evaluations and sensitivity analyses, *J. Geophys. Res.*, *98*(D7), 12609–12617.

Haagen-Smit, A. J. (1952), Chemistry and physiology of Los Angeles smog, *Ind. Eng. Chem.*, *44*(6), 1342–1346.

Haagen-Smit, A. J., and M. M. Fox (1954), Photochemical ozone formation with hydrocarbons and automobile exhaust, *J. Air Pollut. Control Assoc.*, *4*, 105–109.

Hanst, P. L., et al. (1975), A spectroscopic study of California smog, *EPA-650/654-675-006* pp., Report submitted by Research Triangle Park, N. C, Calif. Air Resour. Board.

Hanst, P. L., et al. (1982), A long-path infrared study of Los-Angeles smog, *Atmos. Environ.*, *16*(5), 969–981.

Harley, R. A., et al. (2005), Changes in motor vehicle emissions on diurnal to decadal time scales and effects on atmospheric composition, *Environ. Sci. Technol.*, *39*(14), 5356–5362, doi:10.1021/Es048172+.

Husar, R. B., et al. (1977), 3-Dimensional distribution of air-pollutants in Los-Angeles basin, *J. Appl. Meteorol.*, *16*(10), 1089–1096.

Jacob, D. J. (1999), *Introduction to Atmospheric Chemistry*, Princeton Univ. Press, Princeton, N. J., 199–243.

Jacob, D. J., et al. (2010), The Arctic Research of the Composition of the Troposphere from Aircraft and Satellites (ARCTAS) mission: Design, execution, and first results, *Atmos. Chem. Phys.*, *10*(11), 5191–5212, doi:10.5194/acp-10-5191-2010.

Johnson, G. M. (1984), A simple model for predicting the ozone concentration of ambient air, in *Proceedings of the 8th International Clean Air Conference*., *May 7–11*, vol. 2, edited by H. F. Hartmann, et al., pp. 715–731, Clean Air Soc. of Australia and New Zealand, Melbourne, Victoria, Australia.

Kelly, N. A. (1992), A captive-air irradiation study of the response of nitric-acid and peroxyacetyl nitrate to ozone control strategies in Los Angeles, *Atmos. Environ. Part B*, *26*(4), 463–472, doi:10.1016/0957-1272(92)90053-U.

Kok, G. L., et al. (1978), Ambient air measurements of hydrogen-peroxide in California South Coast Air Basin, *Environ. Sci. Technol.*, *12*(9), 1077–1080.

Kok, G. L., et al. (1988), *Measurements of Hydrogen Peroxide and Formaldehyde in Glendora, California*, Report submitted by the National Center for Atmospheric Research, Boulder, CO., Calif. Air Resour. Board.

Kok, G. L., et al. (1990), Measurements of hydrogen-peroxide and formaldehyde in Glendora, California, *Aerosol Sci. Tech.*, *12*(1), 49–55.
Kopczynski, S. L., et al. (1972), Photochemistry of atmospheric samples in Los Angeles, *Environ. Sci. Technol.*, *6*(4), 342–347.
Lawson, D. R. (1990), The Southern California Air-Quality Study, *J. Air Waste Manage.*, *40*(2), 156–165.
Lawson, D. R. (2003), The weekend ozone effect—The weekly ambient emissions control experiment, *EM Forum*, 17–25.
Lawson, D. R., et al. (1990), Emissions from in-use motor vehicles in Los Angeles—A pilot-study of remote-sensing and the inspection and maintenance program, *J. Air Waste Manage.*, *40*(8), 1096–1105.
Lee, M. H., et al. (2000), Hydrogen peroxide and organic hydroperoxide in the troposphere: A review, *Atmos. Environ.*, *34*(21), 3475–3494.
Leighton, P. A. (1961), *Photochemistry of Air Pollution*, Academic, New York, 1–278.
Leonard, M. J., et al. (1976), Effects of motor vehicle control program on hydrocarbon concentrations in central Los Angeles atmosphere, *J. Air Pollut. Contr. Assoc.*, *26*(4), 359–363.
Lin, X., et al. (1988), On the nonlinearity of the tropospheric ozone production, *J. Geophys. Res.*, *93*(D12), 15879–15888.
Liu, S. C., et al. (1987), Ozone production in the rural troposphere and the implications for regional and global ozone distributions, *J. Geophys. Res.*, *92*(D4), 4191–4207.
Lonneman, W. A., et al. (1968), Aromatic hydrocarbons in the atmosphere of the Los Angeles basin, *Environ. Sci. Technol.*, *2*(11), 1017–1020.
Lonneman, W. A., et al. (1976), PAN and oxidant measurement in ambient atmospheres, *Environ. Sci. Technol.*, *10*(4), 374–380.
Mackay, G. I. (1988), *The Southern California air quality study: Tunable diode laser absorption spectrometer measurements of H_2O_2 and H_2CO at the Claremont and Long Beach "A" sites*, Report submitted by Unisearch Associates, Inc., Calif. Air Resour. Board, Sacramento, *A732-041*, 1–8.
Mackay, G. I. (1994), *Claremont Atmospheric Free-Radical Study: Measurements of Formaldehyde, Hydrogen Peroxide, Nitric Acid, Nitrous Acid, Peroxyacetyl Nitrate, Nitrogen Dioxide, Nitrogen Oxides, Ozone, Carbon Monoxide, Hydrocarbons (C1–C12), and Carbonyl Compounds (C1-Benzaldehyde)*, Report submitted by Unisearch Associates, Inc., Calif. Air Resour. Board, Sacramento, *A92-327*, 1–42.
Mackay, G. I., et al. (1988), *The Southern California Air Quality Study: Tunable Diode Laser Absorption Spectrometer Measurements of HNO3 at the Claremont "A" Site*, Report submitted by Unisearch Associates, Inc., Calif. Air Resour. Board, Sacramento, A732-073, 1–22.
Mackay, G. I., et al. (1990), Measurements of H_2O_2 and HCHO by tunable diode-laser absorption-spectroscopy during the 1986 Carbonaceous Species Methods Comparison Study in Glendora, California, *Aerosol Sci. Tech.*, *12*(1), 56–63.
McDonald, B. C., et al. (2012), Long-term trends in nitrogen oxide emissions from motor vehicles at national, state, and air basin scales, *J. Geophys. Res.*, *117*, D00V18, doi:10.1029/2012JD018304.
Murphy, J. G., et al. (2007), The weekend effect within and downwind of Sacramento—Part 1: Observations of ozone, nitrogen oxides, and VOC reactivity, *Atmos. Chem. Phys.*, *7*(20), 5327–5339, doi:10.5194/acp-7-5327-2007.
Neligan, R. E. (1962), Hydrocarbons in Los-Angeles atmosphere—A comparison between hydrocarbons in automobile exhaust and those found in Los Angeles atmosphere, *Arch. Environ. Health*, *5*(6), 581–591.
Parrish, D. D., et al. (1993), The total reactive oxidized nitrogen levels and the partitioning between the individual species at 6 rural sites in eastern North America, *J. Geophys. Res.*, *98*(D2), 2927–2939.
Parrish, D. D., et al. (2002), Decadal change in carbon monoxide to nitrogen oxide ratio in U.S. vehicular emissions, *J. Geophys. Res.*, *107*(D12), 4140, doi:10.1029/2001JD000720.
Parrish, D. D., et al. (2004), Intercontinental Transport and Chemical Transformation 2002 (ITCT 2K2) and Pacific Exploration of Asian Continental Emission (PEACE) experiments: An overview of the 2002 winter and spring intensives, *J. Geophys. Res.*, *109*, D23S01, doi:10.1029/2004jd004980.
Parrish, D. D., et al. (2011), Air quality progress in North American megacities: A review, *Atmos. Environ.*, *45*(39), 7015–7025, doi:10.1016/j.atmosenv.2011.09.039.
Pollack, I. B., et al. (2012), Airborne and ground-based observations of a weekend effect in ozone, precursors, and oxidation products in the California South Coast Air Basin, *J. Geophys. Res.*, *117*, D00V05, doi:10.1029/2011jd016772.
Press, W. H., et al. (1988), *Numerical Recipes in C*, Cambridge Univ. Press, Cambridge, U. K., 773–839.
Renzetti, N. A., and R. J. Bryan (1961), Atmospheric sampling for aldehydes and eye irritation in Los Angeles smog—1960, *J. Air Pollut. Contr. Assoc.*, *11*(9), 421–427.
Roberts, J. M., et al. (1995), Relationships between PAN and ozone at sites in eastern North America, *J. Geophys. Res.*, *100*(D11), 22821–22830.
Roberts, J. M., et al. (2007), Measurements of PANs during the New England Air Quality Study 2002, *J. Geophys. Res.*, *112*, D20306, doi:10.1029/2007JD008667.
Russell, A. G., et al. (1988a), Mathematical-modeling of the formation of nitrogen-containing air-pollutants.1. Evaluation of an Eulerian photochemical model, *Environ. Sci. Technol.*, *22*(3), 263–270.
Russell, A. G., et al. (1988b), Mathematical-modeling of the formation of nitrogen-containing pollutants. 2. Evaluation of the effect of emission controls, *Environ. Sci. Technol.*, *22*(11), 1336–1347, doi:10.1021/Es00176a014.
Ryerson, T. B., et al. (1998), Emissions lifetimes and ozone formation in power plant plumes, *J. Geophys. Res.*, *103*(D17), 22569–22583.
Ryerson, T. B., et al. (2001), Observations of ozone formation in power plant plumes and implications for ozone control strategies, *Science*, *292*(5517), 719–723, doi:10.1126/science.1058113.
Ryerson, T. B., et al. (2013), The 2010 California Research at the Nexus of Air Quality and Climate Change (CalNex) field study, *J. Geophys. Res.*, doi:10.1002/jgrd.50331.
Sakugawa, H., and I. R. Kaplan (1990), Observation of the diurnal-variation of gaseous H_2O_2 in Los Angeles air using a cryogenic collection method, *Aerosol Sci. Tech.*, *12*(1), 77–85.
Sakugawa, H., et al. (1990), Atmospheric hydrogen peroxide, *Environ. Sci. Technol.*, *24*(10), 1452–1462.
Sander, S. P., et al. (2006), Chemical kinetics and photochemical data for use in atmospheric studies, *JPL Publ. 06-2*, Jet Propul. Lab., Pasadena, Calif.
Sillman, S. (1991), A numerical-solution for the equations of tropospheric chemistry based on an analysis of sources and sinks of odd hydrogen, *J. Geophys. Res.*, *96*(D11), 20735–20744.
Sillman, S. (1995), The use of NO_y, H_2O_2, and HNO_3 as indicators for ozone-NO_x-hydrocarbon sensitivity in urban locations, *J. Geophys. Res.*, *100*(D7), 14175–14188.
Sillman, S., et al. (1990), The sensitivity of ozone to nitrogen oxides and hydrocarbons in regional ozone episodes, *J. Geophys. Res.*, *95*(D2), 1837–1851.
Singer, B. C., et al. (1998), Scaling of infrared remote sensor hydrocarbon measurements for motor vehicle emission inventory calculations, *Environ. Sci. Technol.*, *32*(21), 3241–3248.
Singh, H. B., et al. (1981), Measurements of some potentially hazardous organic chemicals in urban environments, *Atmos. Environ.*, *15*(4), 601–612.
Soltic, P., and M. Weilenmann (2003), NO_2/NO emissions of gasoline passenger cars and light-duty trucks with Euro-2 emission standard, *Atmos. Environ.*, *37*(37), 5207–5216, doi:10.1016/j.atmosenv.2003.05.003.
Spicer, C. W. (1977a), Photochemical atmospheric pollutants derived from nitrogen oxides, *Atmos. Environ.*, *11*(11), 1089–1095.
Spicer, C. W. (1977b), The fate of nitrogen oxides in the atmosphere, in *Advances in Environmental Science and Technology*, edited by J. N. Pitts, et al., John Wiley, New York, 163–261.
Spicer, C. W. (1983), Smog chamber studies of NO_x transformation rate and nitrate precursor relationships, *Environ. Sci. Technol.*, *17*(2), 112–120, doi:10.1021/Es00108a010.
Stedman, D. H., et al. (2009), On-road motor vehicle emissions including NH_3, SO_2 and NO_2 ARB Report.
Stephens, E. R. (1969), The formation, reactions, and properties of peroxyacyl nitrates (PANs) in photochemical air pollution, *Adv. Environ. Sci. Technol.*, *1*, 119–146.
Tanner, R. L., and J. Shen (1990), Measurement of hydrogen-peroxide in ambient air by impinger and diffusion scrubber, *Aerosol Sci. Technol.*, *12*(1), 86–97.
Taylor, J. R. (1997), *An Introduction to Error Analysis: The Study of Uncertainties in Physical Measurements*, 2nd ed., Univ. Sci. Books, Sausalito, Calif, 45–208.
Temple, P. J., and O. C. Taylor (1983), World-wide ambient measurements of peroxyacetyl nitrate (PAN) and implications for plant injury, *Atmos. Environ.*, *17*(8), 1583–1587.
Tonse, S. R., et al. (2008), A process-analysis based study of the ozone weekend effect, *Atmos. Environ.*, *42*(33), 7728–7736, doi:10.1016/j.atmosenv.2008.05.061.
Trainer, M., et al. (1993), Correlation of ozone with NO_y in photochemically aged air, *J. Geophys. Res.*, *98*(D2), 2917–2925.
Tuazon, E. C., et al. (1981), Trace pollutant concentrations in a multiday smog episode in the California South Coast Air Basin by long path-length Fourier-transform infrared-spectroscopy, *Environ. Sci. Technol.*, *15*(10), 1232–1237.
Tuazon, E. C., et al. (1991), Thermal decomposition of peroxyacetyl nitrate and reactions of acetyl peroxy radicals with NO and NO_2 over the temperature range 283–313 K, *J. Phys. Chem.*, *95*(6), 2434–2437.
Warneke, C., et al. (2012), Multiyear trends in volatile organic compounds in Los Angeles, California: Five decades of decreasing emissions, *J. Geophys. Res.*, *117*, D00V17, doi:10.1029/2012JD017899.
Williams, E. L., and D. Grosjean (1990), Southern California Air Quality Study: Peroxyacetyl nitrate, *Atmos. Environ.*, *24A*(9), 2369–2377.
Winer, A. M., et al. (1974), Response of commercial chemiluminescent NO-NO_2 analyzers to other nitrogen-containing compounds, *Environ. Sci. Technol.*, *8*(13), 1118–1121.
Winer, A. M., et al. (1986), Absolute measurements of nitric acid by kilometer pathlength FTIR spectroscopy and their intercomparison with other measurement methods, Calif. Air Resour. Board, University of California, Riverside, A5-051-032.